

Energy and width of a narrow $I = 1/2$ DNN quasibound state

M. Bayar,^{1,2} C. W. Xiao,¹ T. Hyodo,³ A. Doté,^{4,5} M. Oka,^{3,5} and E. Oset¹

¹*Departamento de Física Teórica and IFIC, Centro Mixto Universidad de Valencia-CSIC, Institutos de Investigación de Paterna, Aptdo. 22085, 46071 Valencia, Spain*

²*Department of Physics, Kocaeli University, 41380 Izmit, Turkey*

³*Department of Physics, Tokyo Institute of Technology, Meguro 152-8551, Japan*

⁴*High Energy Accelerator Research Organization (IPNS/KEK), 1-1 Ooho, Tsukuba, Ibaraki, Japan, 305-0801*

⁵*J-PARC Branch, KEK Theory Center, Institute of Particle and Nuclear Studies, High Energy Accelerator Research Organization (KEK), 203-1, Shirakata, Tokai, Ibaraki, 319-1106, Japan*

(Received 29 May 2012; revised manuscript received 27 July 2012; published 31 October 2012)

The energies and widths of DNN quasibound states with isospin $I = 1/2$ are evaluated in two methods, the fixed center approximation to the Faddeev equation and the variational method approach to the effective one-channel Hamiltonian. The DN interactions are constructed so they dynamically generate the $\Lambda_c(2595)$ ($I = 0$, $J^\pi = 1/2^-$) resonance state. We find that the system is bound by about 250 MeV from the DNN threshold, $\sqrt{s} \sim 3500$ MeV. Its width, including both the mesonic decay and the D absorption, is estimated to be about 20–40 MeV. The $I = 0$ DN pair in the DNN system is found to form a cluster that is similar to the $\Lambda_c(2595)$.

DOI: [10.1103/PhysRevC.86.044004](https://doi.org/10.1103/PhysRevC.86.044004)

PACS number(s): 21.45.-v, 14.40.Lb

I. INTRODUCTION

The interaction of mesons with nuclei and the property of mesonic bound states are one of the most important topics in nuclear-hadron physics [1–6]. Bound states of pions and K^- have been investigated for a long time and have revealed the role of strong interactions in the hadron-nucleus bound states. A step forward in the experimental observation of the most deeply bound pionic states was given using the ($d, {}^3\text{He}$) reaction [7], and, although less clearly, using the coherent radiative π^- capture [8] in Ref. [9]. The deeply bound kaon atoms had been studied theoretically using the optical potentials [10–14]. Because of the large imaginary part, the width of the bound states is larger than the energy separation between the levels [5,15], so experimental observation is not feasible (see also Refs. [16,17]).

The simplest of the many-body kaonic nuclear systems is $\bar{K}NN$, which has received much attention theoretically. Because the $\Lambda(1405)$ resonance is interpreted as a quasibound state of the $\bar{K}N$ system in the $\pi\Sigma$ continuum [18–25], one expects a quasibound $\bar{K}NN$ system driven by the attractive $\bar{K}N$ interaction in the isospin $I = 0$ channel. Various approaches have resulted in a rather general consensus that the quasibound state is obtained above the $\pi\Sigma N$ threshold and the width is larger than the binding [26–37]. Thus, the experimental identification of this system would be difficult.

What we report here is the analogous state of the $\bar{K}NN$, substituting the \bar{K} by a D meson. The DN interaction in $I = 0$ is predicted to be attractive in the vector-meson exchange picture and, thus, to dynamically generate the $J^P = 1/2^-$ excited state, $\Lambda_c(2595)$ [38–41]. The $\Lambda_c(2595)$ resonance is rather narrow ($\Gamma < 1.9$ MeV), in contrast to the analogous $\Lambda(1405)$ with apparent widths of the order of 30–60 MeV [23–25]. While the large width of the $\Lambda(1405)$ is responsible for the large width of the $\bar{K}NN$ state, the analogous state DNN , where the $\Lambda_c(2595)$ plays the role of the $\Lambda(1405)$ in

the $\bar{K}NN$ state, has much better chances to survive as a long lived and observable state.

The interaction of the D mesons with nuclei has been addressed in Refs. [39,41,42] and the possibility of making bound atomic states of D mesons in nuclei has been considered in Ref. [43]. The interaction of DN is attractive both in isospin $I = 0$ and $I = 1$, but much weaker for $I = 1$. Although this leads to a weakly attractive D^+p interaction, the Coulomb repulsion becomes important for heavier nuclei. As a consequence, the D will be only weakly bound in heavy nuclei and the probability to see these bound states is not excessively promising [43]. However, few-body systems like DNN are less affected by the Coulomb repulsion particularly for the total isospin $I_{\text{tot}} = 1/2$.

With this in mind we tackle the DNN system from two different approaches. The first one is using the fixed center approximation (FCA) to the Faddeev equations, as done in Refs. [34–36] for the $\bar{K}NN$ system. The second one is using the variational method as done in Refs. [29,30]. In order to gain confidence that the state found is narrow, we have also evaluated the width of the state coming from the absorption of the D by a pair of nucleons going to the $\Lambda_c N$ system in the FCA, analogous to the absorption of \bar{K} by a pair of nucleons as considered in Refs. [11,30,44]. In the variational approach, we extract the typical size of the quasibound state from the obtained wave function.

The paper is organized as follows. In Sec. II, we briefly introduce the coupled-channels approach for the DN scattering and derive the corresponding DN potential. These provide the basis of the three-body calculations in later sections. The FCA to the Faddeev equations is formulated in Sec. III, together with the evaluation of the two-nucleon absorption. The variational approach to the same DNN system is discussed in Sec. IV. The numerical results of the three-body calculations are shown in Sec. V. Discussion of the obtained results is given in Sec. VI. The conclusions of this study are drawn in the last section.

II. DN SCATTERING AND INTERACTION

We consider the two-body DN scattering based on the model in Ref. [39]. This is a coupled-channels approach to the s -wave meson-baryon scattering in the vector-meson exchange picture. The negative parity $\Lambda_c(2595)$ resonance is dynamically generated as a quasibound state of the DN system in the $I = 0$ channel, just like the $\Lambda(1405)$ resonance in the strangeness sector [19–25]. In Sec. II A, we derive the DN two-body scattering amplitude which will be used in the FCA calculation. An effective single-channel potential is constructed to reproduce the equivalent scattering amplitude in Sec. II B. This will be the basic input in the variational calculation. We work in the isospin symmetric limit, which is sufficient for the required precision of the present study.

A. Coupled-channels model for the DN scattering

We consider seven (eight) coupled channels in the isospin $I = 0$ ($I = 1$) sector, DN , $\pi\Sigma_c$, $\eta\Lambda_c$, $K\Sigma_c$, $K\Sigma'_c$, $D_s\Lambda$, and $\eta'\Lambda_c$ (DN , $\pi\Lambda_c$, $\pi\Sigma_c$, $\eta\Sigma_c$, $K\Sigma_c$, $K\Sigma'_c$, $D_s\Sigma$, and $\eta'\Sigma_c$). In Ref. [39], the coupled-channels interaction is given by the Weinberg-Tomozawa term

$$v_{ij}^{(I)}(W) = -\frac{\kappa C_{ij}^{(I)}}{4f^2}(2W - M_i - M_j)\sqrt{\frac{M_i + E_i}{2M_i}}\sqrt{\frac{M_j + E_j}{2M_j}},$$

where W is the total energy, f is the meson decay constant, M_i and E_i are the mass and energy of the baryon in channel i , respectively, and $C_{ij}^{(I)}$ is the group theoretical coupling strength for isospin I . The reduction factor κ is introduced to take into account the mass difference of the exchanged meson, which we set $\kappa = 1$ ($\kappa = \kappa_c = 1/4$) for the uds (charm) flavor exchange process [39]. The scattering amplitude t_{ij} is obtained from the matrix equation

$$t^{(I)} = ((v^{(I)})^{-1} - g^{(I)})^{-1}, \quad (1)$$

where the diagonal loop function is given in dimensional regularization as

$$\begin{aligned} g_i^{(I)}(W; a_i(\mu)) &= \frac{1}{(4\pi)^2} \left\{ a_i(\mu) + \ln \frac{M_i^2}{\mu^2} + \frac{m_i^2 - M_i^2 + W^2}{2W^2} \ln \frac{m_i^2}{M_i^2} \right. \\ &+ \frac{\bar{q}_i}{W} \left[\ln(W^2 - (M_i^2 - m_i^2) + 2W\bar{q}_i) \right. \\ &+ \ln(W^2 + (M_i^2 - m_i^2) + 2W\bar{q}_i) \\ &- \ln(-W^2 + (M_i^2 - m_i^2) + 2W\bar{q}_i) \\ &\left. \left. - \ln(-W^2 - (M_i^2 - m_i^2) + 2W\bar{q}_i) \right] \right\}, \end{aligned}$$

where \bar{q}_i is the magnitude of the three-momentum in the center-of-mass frame. We choose the subtraction constants at $\mu = 1$ GeV as

$$a_{DN} = -2.056, \quad a_i = -2.06 \quad (i \neq DN), \quad (2)$$

for both the $I = 0$ and $I = 1$ states, so the $\Lambda_c(2595)$ resonance is dynamically generated at the observed energy. By choosing the isospin symmetric subtraction constants (2), a resonance

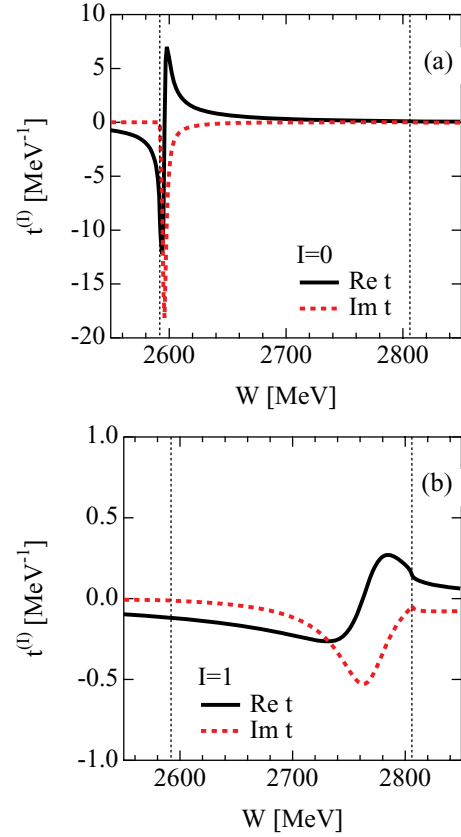


FIG. 1. (Color online) S -wave DN scattering amplitude in the coupled-channels model (1); (a) $I = 0$ channel, (b) $I = 1$ channel. Vertical dotted lines represent the threshold energies of $\pi\Sigma_c$ and DN channels.

state is also generated in $I = 1$ at ~ 2760 MeV. The diagonal components of the s -wave scattering amplitudes in the DN channel, which are complex above the πY_c ($Y_c = \Lambda_c, \Sigma_c$) threshold, are shown in Fig. 1. The resonant nature of the amplitudes can be seen in both channels.

It is worth comparing the $I = 0$ DN - $\pi\Sigma_c$ system with the corresponding $\bar{K}N$ - $\pi\Sigma$ system. Both systems have a quasi-bound state. Neglecting the small effect of the normalization factor, we can write the coupling strength for the DN case as

$$v_{ij} \sim \begin{pmatrix} 3 & \sqrt{\frac{3}{2}}\kappa_c \\ \sqrt{\frac{3}{2}}\kappa_c & 4 \end{pmatrix} \frac{2W - M_i - M_j}{4f^2},$$

where the channels are assigned as DN ($i = 1$) and $\pi\Sigma_c$ ($i = 2$). This is the same form as with the $\bar{K}N$ - $\pi\Sigma$ case, except for the factor $\kappa_c = 1/4$ in the off-diagonal channel. The diagonal interaction is proportional to the meson energy $W - M_i$, which is reduced to the meson mass at threshold. Thus, there are three differences from the strangeness sector: (1) heavy mass of D meson, which enhances the strength of the DN interaction by the energy factor $W - M_i$; (2) large reduced mass of the system, which suppresses the kinetic energy in the charm sector; (3) weak transition coupling $DN \rightarrow \pi\Sigma_c$, which suppresses the decay of the quasibound state into the $\pi\Sigma_c$ state. These facts explain the reason why the

DN quasibound state is generated with larger binding energy and narrower width than those of the $\bar{K}N$ quasibound state. In addition, (1) and (2) also enhance the attractive interaction in the $I = 1$ channel. As a consequence, we obtain a resonance state also in $I = 1$ at ~ 2760 MeV, as far as choosing the isospin symmetric subtraction constants (2).

B. Effective single-channel DN potential

We now construct an effective single-channel potential, which will be used in the variational calculation of the DNN system. We utilize the method in Ref. [45], first constructing a single-channel framework which is equivalent to Eq. (1) and then translating the result into a local and energy-dependent potential in coordinate space.

The effective interaction v^{eff} is constructed to reproduce the original amplitude t_{11} , given by the DN single-channel scattering equation (we suppress the isospin index in this section)

$$t_{11} = [(v^{\text{eff}})^{-1} - g_1]^{-1}. \quad (3)$$

It is shown that the v^{eff} is given by the sum of the bare interaction in channel 1 (v_{11}) and the term with coupled-channels effects as [45]

$$v^{\text{eff}} = v_{11} + \sum_{m=2}^N v_{1m} g_m v_{m1} + \sum_{m,l=2}^N v_{1m} g_m t_{ml}^{(N-1)} g_l v_{l1}, \quad (4)$$

where $t_{ml}^{(N-1)} = [(v^{(N-1)})^{-1} - g^{(N-1)}]^{-1}$ is the $(N-1) \times (N-1)$ matrix of the coupled-channels amplitude without the DN channel. In this way, Eq. (3) gives the equivalent amplitude with the 11 components in Eq. (1). v^{eff} is complex above the πY_c threshold, because of the imaginary part of the loop function of the πY_c channel in Eq. (4).

We then translate v^{eff} into the local potential in coordinate space. Adopting a single Gaussian form for the spatial distribution, the two-body potential can be written as

$$v_{DN}(r; W) = \frac{M_N}{2\pi^{3/2} a_s^3 \tilde{\omega}(W)} [v^{\text{eff}}(W) + \Delta v(W)] \exp[-(r/a_s)^2], \quad (5)$$

where $a_s = 0.4$ fm is the range parameter of the potential and $\tilde{\omega}(W)$ is the reduced energy of the DN system. The energy-dependent correction term $\Delta v(W)$ is introduced to compensate the deviation from the local potential approximation. This complex and energy-dependent potential reproduces the scattering amplitude t_{11} when the Schrödinger equation with this potential is self-consistently solved. The strength of the potential $v_{DN}(r; W)$ at $r = 0$ is shown in Fig. 2. One finds that the real part (imaginary part) is larger (smaller) than that of the $\bar{K}N$ potential [45], which demonstrates the differences of the interaction kernel discussed in the previous section.

III. THE FIXED-CENTER APPROXIMATION FOR THE DNN SYSTEM

The fixed-center approximation (FCA) to the Faddeev equations has been used with success in several problems.

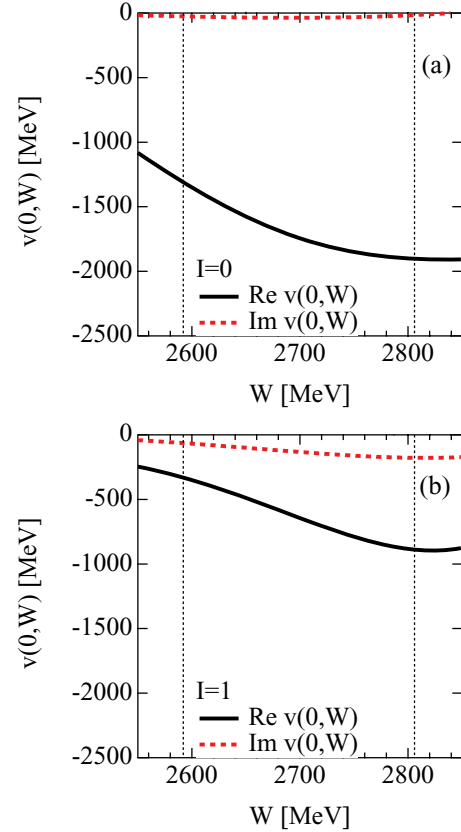


FIG. 2. (Color online) Strength of the effective potential $v_{DN}(r, W)$ at $r = 0$ by Eq. (5); (1) $I = 0$ channel, (b) $I = 1$ channel. The range parameter is chosen to be $a_s = 0.4$ fm. Vertical dotted lines represent the threshold energies of $\pi \Sigma_c$ and DN channels.

It is advantageous in that the two-body absorption process of the three-body system can be calculated as discussed in Sec. III B. One assumes that a pair of particles remains relatively unaffected by the interaction of the third particle with this pair. This usually happens when the third particle is lighter than the constituents of the pair and also if the cluster is tightly bound. The method has been used with success in the study of K^- scattering with the deuteron in Refs. [46–49] (see a review in Ref. [50] for comparison with full Faddeev calculations). More recently, it has been applied to systems of two mesons and a baryon in Ref. [51], where the $N\bar{K}K$ system is investigated. The results obtained are in good agreement with more accurate results obtained with variational calculations in Ref. [52] or the Faddeev equations in coupled channels [53,54]. The puzzle of the $\Delta_{5/2^+}(2000)$ is also addressed with this technique, assuming this resonance to be mostly built up from $\pi\rho\Delta$ in Ref. [55]. Closer dynamically to the problem under consideration is the work of Ref. [56], where the NDK , $\bar{K}DN$, and $ND\bar{D}$ systems are studied with this method.

In the present case, where we want to study the DNN system, we have also the precedent of the work of Refs. [34,36], where the $\bar{K}NN$ system was studied within this approximation and found to provide results in qualitative agreement with those of the variational calculations [29,30]. The condition that the interacting particle (D meson) is lighter than those of the

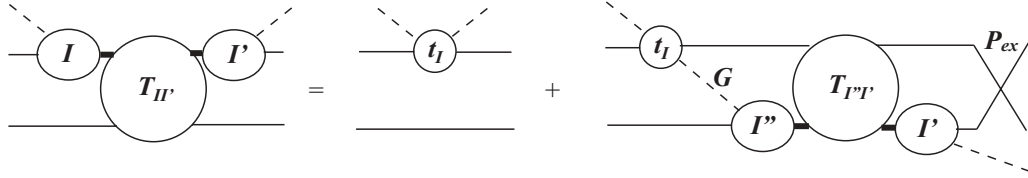


FIG. 3. Diagrammatic illustration of the three-body equation (6).

two-body cluster (nucleon) is not fulfilled in this case. This certainly introduces larger uncertainties than in other cases studied but we still expect that one can get good results at a qualitative level. Actually, the real difficulty of the FCA occurs when one applies it to studying possible resonant three-body systems above the threshold of the three particles [57]. In the present case, we look for deeply bound states of the DNN system and we are safer. However, in order to be more certain about the results, we have also performed calculations using a variational method. The differences found in the two approaches can give us an idea of the uncertainties, and the features shared by the two approaches can be considered more reliable.

The work of Ref. [57] gives us some idea of when we should expect a break down of the FCA. Indeed, in that work the system $\phi K \bar{K}$ was studied within the FCA with the system $K \bar{K}$ forming the cluster on which the ϕ collides. The results were compared with a full Faddeev calculation [58] where the $\phi(2170)$ resonance was dynamically generated, with the $K \bar{K}$ system clustering around the $f_0(980)$ resonance. The comparison of two approaches allowed one to see that the FCA was failing to provide realistic results because it did not allow the $K \bar{K}$ system to be excited in intermediate states. Since the energy of the system is 90 MeV above the threshold of its components, the ϕ , a massive particle compared to the mass of the components of the cluster, can easily produce excited intermediate states of the $K \bar{K}$ system in its collisions with the kaons and this is accounted for by the Faddeev calculations of Ref. [58] but not in the FCA, where the $K \bar{K}$ cluster wave function is supposed to be unaltered. Maintaining the structure of the cluster on collisions can happen either when the interacting particle with the cluster is very light or in the case when it is not light (like in the present case), when the system is rather bound such that the interacting particle does not have energy to excite the cluster. The situation for the DNN case that we study corresponds to this latter case and we expect a fair description of the three-body system within the FCA.

A. The formalism for the FCA in the DNN system

In the FCA to the Faddeev equations for the DNN three-body system, one takes the NN as a cluster and D scatters from that cluster. We consider the DNN system with total isospin $I_{\text{tot}} = 1/2$ and with the total spin-parity $J^P = 0^-$ and $J^P = 1^-$. In this approach, all the two-body pairs are in s wave.

First, we make the evaluation for the case of $J^P = 0^-$, which corresponds to the spin (isospin) of the NN pair as $S_{NN} = 0$ ($I_{NN} = 1$). To have total isospin $I_{\text{tot}} = 1/2$, the dominant component of the DN system is $I = 0$, where the $\Lambda_c(2595)$ resonance appears.

The T matrix for the three-body DNN scattering is labeled by the DN isospins in the entrance channel I and the exit channel I' , $T_{I,I'}$. We denote the two-body (s -wave) DN scattering amplitudes by $t^{(0)}$ for $I = 0$ and $t^{(1)}$ for $I = 1$. The T matrix then satisfies

$$T_{I,I'} = t^{(I)} \delta_{I,I'} + t^{(I)} G_{I,I'} G_0 T_{I',I'} P_{\text{ex}}, \quad (6)$$

which is diagrammatically represented in Fig. 3. In Eq. (6), G_0 is the meson exchange propagator [34,59]

$$G_0 = \int \frac{d^3q}{(2\pi)^3} F_{NN}(q) \frac{1}{q^{02} - \vec{q}^2 - m_D^2 + i\epsilon}, \quad (7)$$

where $F_{NN}(q)$ is the form factor, representing the momentum distribution of the NN system. P_{ex} is the isospin exchange factor, which depends on the total isospin of the nucleons, I_{NN} , in the final state, $P_{\text{ex}} = (-1)^{I_{NN}+1} = 1$ for $J = 0$, and $= -1$ for $J = 1$.

Here we concentrate on the isospin factors in the DNN scattering amplitudes. We define the isospin doublets, $N = (p, n)$, $D = (D^+, -D^0)$ and consider the DNN states with the total isospin $I_{\text{tot}} = 1/2$. There are two independent states with the total spin $J = 0$ and $J = 1$, which can be decomposed into the DN isospin eigenstates, as

$$\begin{aligned} |D(N_1 N_2)_{I_{NN}=1}\rangle_{J=0} &= \frac{\sqrt{3}}{2} |(DN_1)_0 N_2\rangle + \frac{1}{2} |(DN_1)_1 N_2\rangle, \\ |D(N_1 N_2)_{I_{NN}=0}\rangle_{J=1} &= -\frac{1}{2} |(DN_1)_0 N_2\rangle + \frac{\sqrt{3}}{2} |(DN_1)_1 N_2\rangle. \end{aligned}$$

The D exchange matrix is given in terms of the isospin recombination factors.

$$\begin{aligned} |(DN_1)_0 N_2\rangle &= \frac{1}{2} |(DN_2)_0 N_1\rangle + \frac{\sqrt{3}}{2} |(DN_2)_1 N_1\rangle, \\ |(DN_1)_1 N_2\rangle &= \frac{\sqrt{3}}{2} |(DN_2)_0 N_1\rangle - \frac{1}{2} |(DN_2)_1 N_1\rangle. \end{aligned}$$

Thus, the transition matrix G is given by

$$G = \begin{pmatrix} \frac{1}{2} & \frac{\sqrt{3}}{2} \\ \frac{\sqrt{3}}{2} & -\frac{1}{2} \end{pmatrix}.$$

The three-body amplitude $T_{I,I'}$ is obtained by solving Eq. (6),

$$\begin{aligned} T &= \left[1 - \frac{1}{2} (t^{(0)} - t^{(1)}) G_0 P_{\text{ex}} - t^{(0)} t^{(1)} G_0^2 \right]^{-1} \\ &\times \begin{pmatrix} t^{(0)} + \frac{1}{2} t^{(1)} G_0 t^{(0)} P_{\text{ex}} & \frac{\sqrt{3}}{2} t^{(0)} t^{(1)} G_0 P_{\text{ex}} \\ \frac{\sqrt{3}}{2} t^{(0)} t^{(1)} G_0 P_{\text{ex}} & t^{(1)} - \frac{1}{2} t^{(0)} G_0 t^{(1)} P_{\text{ex}} \end{pmatrix}. \end{aligned}$$

In calculating the T matrix for the scatterings in the $J = 0$ and $J = 1$ channels, we take the linear combinations, with a factor 2 for the choice of the first nucleon, as

$$T(J=0) = 2 \begin{pmatrix} \frac{\sqrt{3}}{2} & \frac{1}{2} \\ T_{10} & T_{11} \end{pmatrix} \begin{pmatrix} \frac{\sqrt{3}}{2} \\ \frac{1}{2} \end{pmatrix},$$

$$T(J=1) = 2 \begin{pmatrix} -\frac{1}{2} & \frac{\sqrt{3}}{2} \\ T_{10} & T_{11} \end{pmatrix} \begin{pmatrix} -\frac{1}{2} \\ \frac{\sqrt{3}}{2} \end{pmatrix}.$$

Substituting the T matrix and replacing P_{ex} by $+1$ for $J = 0$, $I_{NN} = 1$ scattering and -1 for $J = 1$, $I_{NN} = 0$, we obtain

$$T(J=0) = \left[\frac{3}{2}t^{(0)} + \frac{1}{2}t^{(1)} + 2t^{(0)}t^{(1)}G_0 \right] \times \left\{ 1 - \frac{1}{2}[t^{(0)} - t^{(1)}]G_0 - t^{(0)}t^{(1)}G_0^2 \right\}^{-1}, \quad (8)$$

$$T(J=1) = \left[\frac{1}{2}t^{(0)} + \frac{3}{2}t^{(1)} + 2t^{(0)}t^{(1)}G_0 \right] \times \left\{ 1 + \frac{1}{2}[t^{(0)} - t^{(1)}]G_0 - t^{(0)}t^{(1)}G_0^2 \right\}^{-1}. \quad (9)$$

These results coincide with those derived in the charge basis [35,36] (see Appendix B).

We can see that Eq. (7) contains the folding of the D intermediate propagator with the form factor of the NN system. The variable q^0 in Eq. (7) is the energy carried by the D , which is given by

$$q^0 = \frac{s + m_D^2 - (2M_N)^2}{2\sqrt{s}},$$

with \sqrt{s} for the rest energy of the DNN system. Equation (7) requires the NN form factor. For $I_{NN} = 0$ one could take the deuteron form factor, but the attraction of the D on the nucleons will make the NN system more compact, like in the case of the $\bar{K}NN$ system. Yet, there are limits on how much one can contract this system because of the strong NN repulsion at short distances. In order to estimate the NN size, one can rely on the results of Ref. [30] in the study of the $\bar{K}NN$ system, where the NN repulsion at short distance was explicitly taken into account. In practical terms we use the same expression for the form factor as for the deuteron [60]

$$F(q) = \int_0^\infty d^3p \sum_{j=1}^{11} \frac{C_j}{\vec{p}^2 + m_j^2} \sum_{i=1}^{11} \frac{C_i}{(\vec{p} - \vec{q})^2 + m_i^2}, \quad (10)$$

but with the parameters m_i rescaled such as to give an average separation of the nucleons of $R_{NN} \simeq 2$ fm [30]. They are shown in Fig. 4. The validity of this NN form factor will be examined by the result of the variational calculation, where the average distance of the NN pair in the DNN system will be optimized in the three-body dynamics.

We need the argument s_1 of the DN amplitude, $t(\sqrt{s_1})$. To evaluate it, we adopt a common procedure of dividing the binding energy into the three particles proportionally to their masses. The energy of the nucleon and the D meson are given by

$$E_N = M_N \frac{\sqrt{s}}{2M_N + m_D}, \quad E_D = m_D \frac{\sqrt{s}}{2M_N + m_D},$$

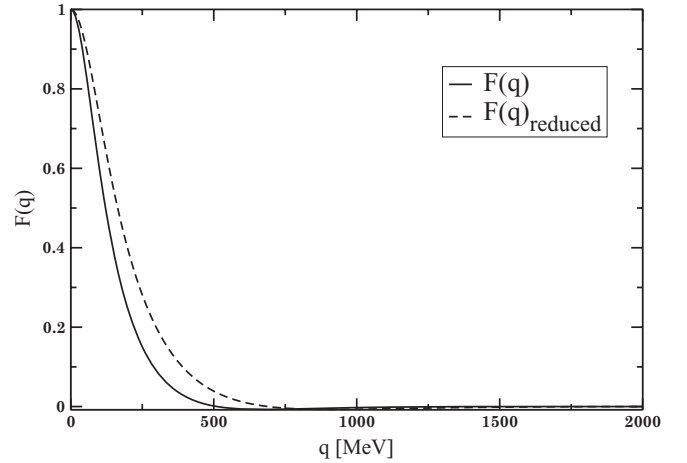


FIG. 4. Form factor of the deuteron and the one corresponding to an NN system with a reduced radius from Ref. [30].

so the total energy of the two-body system can be calculated as

$$s_1 = (p_D + p_{N_1})^2 = s \left(\frac{M_N + m_D}{2M_N + m_D} \right)^2 - \vec{p}_{N_2}^2. \quad (11)$$

The approximate value of $\vec{p}_{N_2}^2$ can be obtained by assuming

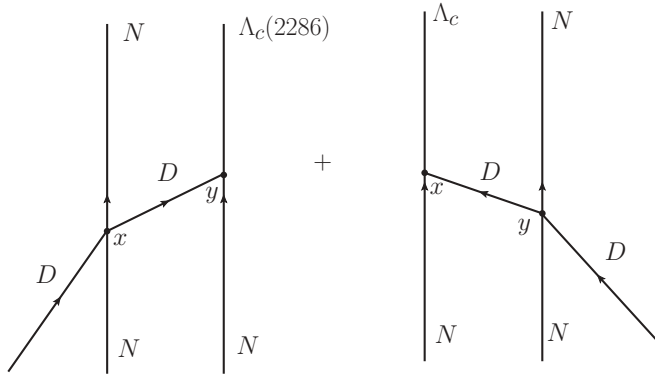
$$\frac{\vec{p}_{N_2}^2}{2M_N} \simeq B_{N_2}; \quad B_{N_2} = M_N - M_N \frac{\sqrt{s}}{2M_N + m_D}, \quad (12)$$

which provides a rough estimate for bound systems with the strong interaction.

We use here a different prescription for s_1 than the one used in Ref. [34]. The latter one was based on the calculation of $s_1 = (p_A + p_1)^2 = m_A^2 + m_{b_1}^2 + 2p_A \cdot p_1$ and further steps to calculate $p_A \cdot p_1$, where A is the interacting particle and b_1 one of the particles of the cluster. However, when the binding of the system is large, like in the present case, assuming $p_A^2 = m_A^2$ and $p_1^2 = m_{b_1}^2$ grossly underestimated the binding of the particles and we have introduced the new, more realistic prescription of Eq. (11).

B. Evaluation of the $D(NN)$ absorption

As we shall see in Sec. V, we obtain a DNN bound system with a very small width. This is related to the small width of the $\Lambda_c(2595)$ state which is generated in DN interaction in $I = 0$. Yet, this calculation only takes into account the decay channel $DN \rightarrow \pi \Sigma_c$, for which there is little phase space, and the $DN \rightarrow \pi \Lambda_c$ channel, which comes from the subdominant $DN I = 1$ component in the DNN system. Now we allow the D to be absorbed by two nucleons, analogously to the $\bar{K}NN \rightarrow \Lambda N$ considered in Refs. [11,44]. Here the channel will be $DNN \rightarrow N \Lambda_c$, whose absorption process is shown diagrammatically in Fig. 5 (other mechanisms and decay channels will be discussed at the end of this section). We calculate only the first diagram in Fig. 5. The second one gives an identical contribution and they sum incoherently: There is no interference since the $N \Lambda_c$ and $\Lambda_c N$ are orthogonal states. Hence, the total width will be twice the one obtained from just one diagram.


 FIG. 5. Diagrammatic representation of the $D(NN)$ absorption.

The S matrix for the diagram is given by

$$\begin{aligned}
 S &= \int d^4x \int d^4y (-i) t_{DN \rightarrow DN} \\
 &\times \frac{1}{\sqrt{2\omega_D}} \varphi_D(\vec{x}) e^{-i\omega_D x^0} e^{iE_{N_1} x^0} e^{-iE_{N_1} x^0} \varphi_{N_1}^*(\vec{x}) \varphi_{N_1}(\vec{x}) \\
 &\times \int \frac{d^4q}{(2\pi)^4} e^{-iq(y-x)} \frac{i}{q^2 - m_D^2 + i\epsilon} \\
 &\times V_y \vec{\sigma} \vec{q} e^{iE_{\Lambda_c} y^0} e^{-iE_{N_2} y^0} \varphi_{\Lambda_c}^*(\vec{y}) \varphi_{N_2}(\vec{y}),
 \end{aligned}$$

where V_y is the Yukawa vertex. We take the same coupling as $K^- p \rightarrow \Lambda$ since in the D and Λ_c the c quark plays the role of the s quark in the \bar{K} and Λ . In Ref. [61], the V_y is given as

$$V_y = -\frac{1}{\sqrt{3}} \frac{3F + D}{2f},$$

with $D = 0.795$, $F = 0.465$ [62]. We perform the x^0, y^0 integrations and make a change of the spatial variables as

$$\vec{x} = \vec{R} - \frac{\vec{r}}{2}, \quad \vec{y} = \vec{R} + \frac{\vec{r}}{2}.$$

We can then write

$$\varphi_{N_1}(\vec{x}) \varphi_{N_2}(\vec{y}) = \frac{1}{\sqrt{V}} e^{i\vec{P} \cdot \vec{R}} \varphi(\vec{r}),$$

where $\varphi(\vec{r})$ is the wave function of the NN system. N_1' and Λ_c will be outgoing plane waves. Let us also assume that the D is a plane wave with a certain momentum. The final formula that we shall use is independent of this momentum, as we shall see. Thus,

$$\varphi_D(\vec{x}) = \frac{1}{\sqrt{V}} e^{i\vec{p}_D \cdot \vec{x}},$$

and then, using these new functions, the S matrix is written as follows:

$$\begin{aligned}
 S &= \frac{1}{V^2} \int \frac{d^3q}{(2\pi)^3} \frac{1}{\sqrt{2\omega_D}} t_{DN \rightarrow DN} \frac{1}{q^2 - m_D^2 + i\epsilon} \\
 &\times V_y \vec{\sigma} \vec{q} \vec{\varphi} \left(\vec{q} - \vec{p}_{\Lambda_c} + \frac{\vec{P}}{2} \right) (2\pi)^4 \delta^4(p_i - p_f) \\
 &\equiv -iT \frac{1}{\sqrt{2\omega_D}} \frac{1}{V^2} (2\pi)^4 \delta^4(p_i - p_f),
 \end{aligned} \tag{13}$$

where $\vec{\varphi}(\vec{q})$ is the Fourier transform of the wave function $\varphi(\vec{r})$ normalized to 1 and p_i and p_f are the initial and final momentum, respectively. The NN wave function in momentum space is defined as

$$\vec{\varphi}(\vec{q}) = \int d^3x e^{i\vec{q} \cdot \vec{x}} \varphi(\vec{x}),$$

and has a maximum value for $\vec{q} = 0$. If we take the NN system at rest, $\vec{P} = 0$, the wave function $\vec{\varphi}(\vec{q})$ in Eq. (13) will peak at $\vec{q} - \vec{p}_{\Lambda_c} = 0$. This allows us to approximate the D propagator in Eq. (13) as

$$\frac{1}{q^2 - m_D^2} \rightarrow \frac{1}{(q^0)^2 - \vec{p}_{\Lambda_c}^2 - m_D^2}, \tag{14}$$

where $q^0 = E_{\Lambda_c} - E_{N_2}$ and $p_{\Lambda_c} \approx \lambda^{1/2}(M_{NN}^2, M_N^2, M_{\Lambda_c}^2)/2M_{NN}$ with $\lambda(M_{NN}^2, M_N^2, M_{\Lambda_c}^2) = M_{NN}^4 + M_N^4 + M_{\Lambda_c}^4 - 2M_{NN}^2 M_N^2 - 2M_{NN}^2 M_{\Lambda_c}^2 - 2M_N^2 M_{\Lambda_c}^2$. We do not need to specify the $t_{DN \rightarrow DN}$ amplitude since it will be accounted for at the end of the formalism.

Defining of $\vec{q} - \vec{p}_{\Lambda_c} \equiv \vec{q}'$, the square of the total matrix element is obtained as follows:

$$\begin{aligned}
 |T|^2 &= V_y^2 \vec{p}_{\Lambda_c}^2 \left(\frac{1}{(q^0)^2 - p_{\Lambda_c}^2 - m_D^2} \right)^2 \\
 &\times \left| \frac{1}{2\pi^2} \int q^2 dq' \vec{\varphi}(\vec{q}') t_{DN, DN}(\sqrt{s'}) \right|^2,
 \end{aligned} \tag{15}$$

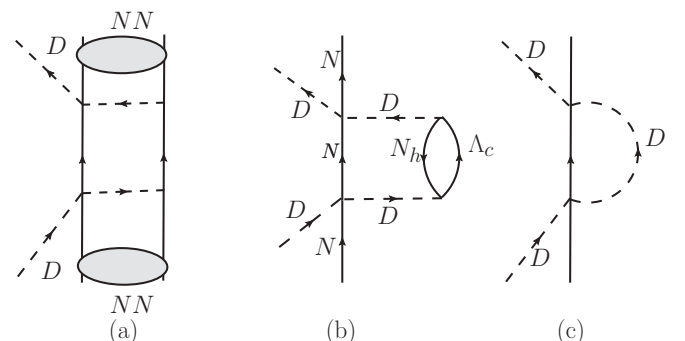
With this T matrix we evaluate the cross section for the process of Fig. 5 (left) and we obtain

$$\sigma_{\text{abs}} = \frac{1}{2\pi} \frac{M_{NN} M_{\Lambda_c} M_N}{M_{NN}^2} \frac{p_{\Lambda_c}}{p_D} |T|^2.$$

It is interesting to relate this cross section to the imaginary part of the forward $D(NN) \rightarrow D(NN)$ amplitude from the diagram of Fig. 6 using the optical theorem. We find

$$\text{Im } T_{D(NN)} = -\frac{p_D \sqrt{s}}{M_{NN}} \sigma_{\text{abs}} = -\frac{1}{2\pi} \frac{M_{\Lambda_c} M_N}{M_{NN}^2} p_{\Lambda_c} |T|^2.$$

The next step is to convert the absorption diagram of Fig. 6(a) into a ‘‘many-body’’ diagram [Fig. 6(b)] where the nucleon where the D is absorbed, the only occupied state of the ‘‘many-body’’ system, is converted into a hole state in the many-body terminology [63]. Once this is done, one observes that if we remove the amplitude t_{DN} in the expression of T ,


 FIG. 6. $D(NN)$ absorption.

the expression that we obtain for $\text{Im } T_{D(NN)}$ corresponds to the evaluation of the imaginary part of the two-body loop function g of a nucleon and a D meson [Fig. 6(c)] but with a D self-energy insertion accounting for the $(\Lambda_c N_h)$ excitation of the D meson. We call this $\delta\tilde{g}$. The Feynman rules to evaluate $\text{Im } \delta\tilde{g}$ and $\text{Im } T_{D(NN)}$ are identical, except that $t_{DN, DN}$ is removed in the evaluation of $\text{Im } \delta\tilde{g}$. Hence, we obtain

$$i\text{Im } \delta\tilde{g} = -i \frac{1}{2\pi} \frac{M_{\Lambda_c} M_N}{M_{NN D}} p_{\Lambda_c} |\tilde{T}|^2.$$

with $|\tilde{T}|^2$ is given by Eq. (15) removing $t_{DN, DN}$. This simplifies the expression since

$$\begin{aligned} \frac{1}{2\pi^2} \int q'^2 dq' \tilde{\varphi}(\vec{q}') &= \lim_{r \rightarrow 0} \int \frac{d^3 q'}{(2\pi)^3} e^{i\vec{q}'\vec{r}} \tilde{\varphi}(\vec{q}') \\ &= \varphi(r=0). \end{aligned} \quad (16)$$

Thus, $|\tilde{T}|^2$ is given by

$$|\tilde{T}|^2 = V_y^2 \vec{p}_{\Lambda_c}^2 \frac{1}{[(q^0)^2 - p_{\Lambda_c}^2 - m_D^2]^2} |\varphi(0)|^2.$$

Finally, $\vec{p}_{\Lambda_c}^2$, accompanying V_y^2 in the former expression, requires a small correction. The factor comes from the nonrelativistic $\vec{\sigma}\vec{q}$ form of the $DN\Lambda_c$ vertex. If we take, instead, the relativistic Yukawa vertex of the type $\gamma^\mu\gamma^5$, then we find the easy prescription to account for the relativistic correction,

$$V_y^2 \vec{p}_{\Lambda_c}^2 \rightarrow V_y^2 \frac{1}{4m_{\Lambda_c}^2} (M_N + M_{\Lambda_c})^2 \vec{p}_{\Lambda_c}^2.$$

The next step is to reevaluate the $t_{DN, DN}$ amplitude used as input in the fixed center formulas. As we mentioned, they were obtained using the method of Ref. [39] with several coupled channels and the formula (1). We redo the evaluation by replacing the loop function in the DN channel as

$$g_{DN} \rightarrow g_{DN} + i\text{Im } \delta\tilde{g} \quad (17)$$

to take into account the D absorption by two nucleons or, analogously, the $\Lambda_c N_h$ excitation of the D meson. When doing this, the DN amplitude becomes complex below the DN threshold and the narrow $\Lambda_c(2595)$ resonance acquires now a moderate width due to the D absorption with a second nucleon. The second process of Fig. 5 (right) is accounted for when we consider the three-body amplitude T in the FCA formula with the first D scattering with the second nucleon.

For the estimation of the width we take the wave function

$$\begin{aligned} \varphi(r) &= ae^{-ar}, \quad a = \frac{1}{2} \left(\frac{\alpha^3}{2\pi} \right)^{\frac{1}{2}}, \\ \tilde{\varphi}(q) &= \frac{4\pi a\alpha}{(\frac{1}{4}\alpha^2 - q^2)^2 + q^2\alpha^2}, \end{aligned}$$

with $\alpha \simeq 1.7 \text{ fm}^{-1}$, which corresponds to an NN object of relative distance 2 fm.

Let us numerically investigate the effect of the absorption using the model described in Sec. II A. In Fig. 7, we show the meson-baryon loop function g_{DN} in the DN channel together with the two-body absorption contribution to the imaginary part, $i\text{Im } \delta\tilde{g}$. We can see that the imaginary part of the total g

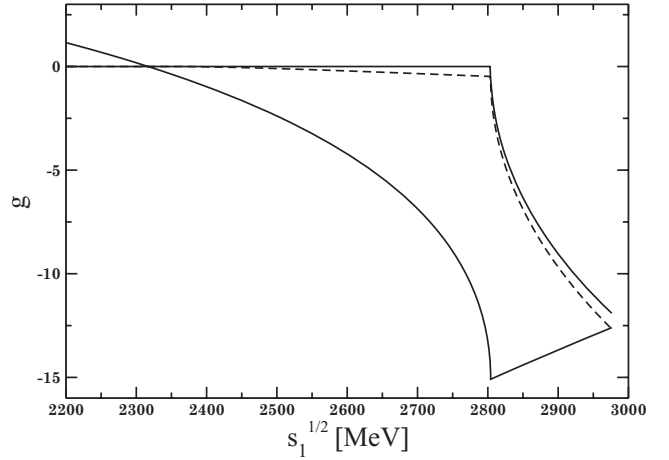


FIG. 7. The meson-baryon loop function g_{DN} in the DN channel (solid line) and with the effect of the two-body absorption $i\text{Im } \delta\tilde{g}$ added (dashed line).

function is no longer zero below the DN threshold due to D absorption. In Fig. 8, we show the modulus of the two-body amplitude $|t|$ for the DN channel for $I=0$ using g_{DN} and $g_{DN} + i\text{Im } \delta\tilde{g}$ of Eq. (17). As we can see, the inclusion of the absorption mechanism induces an increase in the width of the peak of $\Lambda_c(2595)$ in $|t|$ which will have repercussions in the width of the DNN system.

For a narrow resonance, we can approximate the amplitude around the resonance energy by a Breit-Wigner form,

$$t(\sqrt{s_1}) \simeq \frac{g^2}{\sqrt{s_1} - M_R + i\frac{\Gamma}{2}}.$$

This leads to the expression of the coupling of the resonance to the DN scattering state as

$$g^2 = \frac{1}{2} \Gamma |t(M_R)|.$$

Inspection of Fig. 8, together with the values of Γ (no absorption) = 3 MeV and Γ (absorption) = 15 MeV, show that the

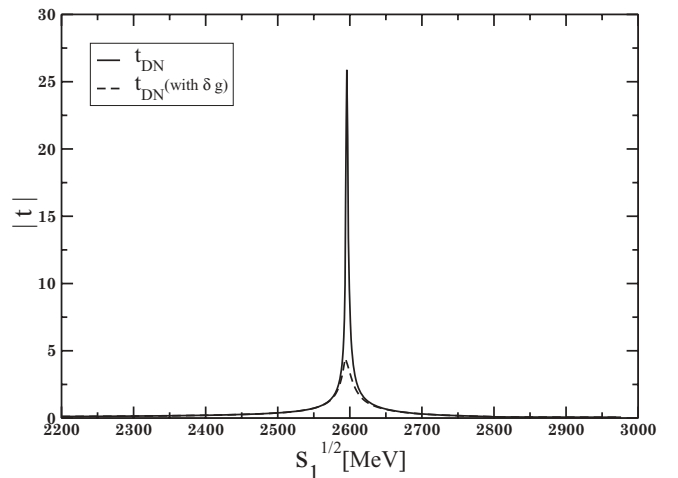


FIG. 8. Modulus of the two-body amplitude $DN \rightarrow DN$ (solid line) and with the effect of the two-body absorption $i\text{Im } \delta\tilde{g}$ added (dashed line).

value of the coupling g^2 barely changes from the introduction of $i\text{Im } \delta\tilde{g}$, but, of course, the resonance has become wider. Indeed, $g^2(\text{noabsorption})/g^2(\text{absorption}) \simeq 6/5$.

The absorption diagram that we have considered is not the only one, but it is the most relevant. On the same footing, we should consider the diagrams where the Yukawa coupling produces Σ_c or even $\Sigma_c^*(2520)$. The analogy with the kaons made before, and the values of these couplings that can be seen in Ref. [62], together with the dynamical factor p^3 of the cross section, make the contribution of these terms of the order of 5% of the Λ_c production and we neglect them. Analogously, we can also have $DN \rightarrow \pi(\eta)\Lambda_c(\Sigma_c)$ in the first hadron line of the absorption diagram and exchange a pion or an η . These diagrams are further suppressed because they require the exchange of a heavy vector in the $DN \rightarrow \pi(\eta)Y_c$ amplitude in the extension of the hidden gauge approach that we use. They are penalized by the factor κ_c^2 , which, even considering that the pion (η) propagators have bigger strength than the D one, renders these diagrams at the level of 10%.

IV. VARIATIONAL CALCULATION OF THE DNN SYSTEM

Here we calculate the energy of the DNN system with a variational approach formulated for the $\bar{K}NN$ system in Refs. [29,30]. As in the case of the FCA, we consider the DNN system with total isospin $I = 1/2$ and the total spin-parity either $J^P = 0^-$ or $J^P = 1^-$. The trial wave function for the $J^P = 0^-$ state is prepared with two components,

$$|\Psi^{J=0}\rangle = (\mathcal{N}^0)^{-1} [|\Phi_+^0\rangle + C^0|\Phi_-^0\rangle],$$

where \mathcal{N}^0 is a normalization constant and C^0 is a mixing coefficient. In the main component $|\Phi_+^0\rangle$, two nucleons are combined into spin $S_{NN} = 0$ and isospin $I_{NN} = 1$ so all the two-body subsystems can be in s wave. We also allow a mixture of the $|\Phi_-^0\rangle$ component where both spin and isospin are set to be zero, so the orbital angular momentum between two nucleons is odd. The $J^P = 1^-$ state is studied in a similar way as

$$|\Psi^{J=1}\rangle = (\mathcal{N}^1)^{-1} [|\Phi_+^1\rangle + C^1|\Phi_-^1\rangle],$$

where $|\Phi_+^1\rangle$ ($|\Phi_-^1\rangle$) denotes the $S_{NN} = 1$ and $I_{NN} = 0$ ($S_{NN} = 1$ and $I_{NN} = 1$) components. Note that only the main component of $|\Phi_+^{J=0,1}\rangle$ is taken into account in the FCA calculation. The wave functions are expanded in terms of Gaussians in coordinate space, and we minimize the total energy of the system with the Hamiltonian given below. Detailed explanation of the variational method can be found in Ref. [30].

We consider the following Hamiltonian in this study:

$$\hat{H} = \hat{T} + \hat{V}_{NN} + \text{Re } \hat{V}_{DN} - \hat{T}_{\text{c.m.}}, \quad (18)$$

where \hat{T} is the total kinetic energy, \hat{V}_{DN} is the DN potential term which is the sum of the contributions from two nucleons, and $\hat{T}_{\text{c.m.}}$ is the energy of the center-of-mass motion. For the NN potential \hat{V}_{NN} , we use three models: HN1R, which is constructed from the Hasegawa-Nagata No. 1 potential [64], the Minnesota force [65], and the Gaussian-fitted version of

the Argonne v18 potential [66]. The characteristic features of these NN potentials are summarized in Appendix A. For later convenience, we define the following matrix elements:

$$\begin{aligned} E_{\text{kin}} &= \langle \Psi | \hat{T} - \hat{T}_{\text{c.m.}} | \Psi \rangle, \\ V(NN) &= \langle \Psi | \hat{V}_{NN} | \Psi \rangle, \\ V(DN) &= \langle \Psi | \text{Re } \hat{V}_{DN} | \Psi \rangle, \\ T_{\text{nuc}} &= \langle \Psi | \hat{T}_N - \hat{T}_{\text{c.m.,}N} | \Psi \rangle, \\ E_{NN} &= T_{\text{nuc}} + V(NN), \end{aligned}$$

where \hat{T}_N and $\hat{T}_{\text{c.m.,}N}$ are nucleonic parts of the kinetic term and center-of-mass energy, respectively.

We take the real part of the DN potential for the energy variation, and the imaginary part will be used to estimate the mesonic decay width. The energy dependence of the interaction was treated self-consistently in the study of $\bar{K}NN$ system [30]. While the $\bar{K}N$ amplitude is well calibrated by experimental data such as total cross sections and $\pi\Sigma$ mass distributions, the DN amplitude is constrained only by the mass of the quasibound state $\Lambda_c(2595) = \Lambda_c^*$. In addition, the self-consistent treatment requires some assumption on the energy fraction of the DN pair in the three-body system, which cannot be determined unambiguously. In this study, therefore, we refrain from the self-consistent treatment of the energy of the DN subsystem and set the strength of the potential at the energy of Λ_c^* resonance,

$$\text{Re } v_{DN}(r=0; W = M_{\Lambda_c^*}) = \begin{cases} -1336 \text{ MeV} & (I = 0) \\ -343 \text{ MeV} & (I = 1) \end{cases}, \quad (19)$$

with $M_{\Lambda_c^*} = 2597.1$ MeV. In this case, the $M_{\Lambda_c^*}$ in $I = 0$ channel is correctly reproduced, while the $I = 1$ resonance disappears, because the strength of the DN potential (5) reduces at the lower energy region, as seen in Fig. 2.

It is useful to introduce one- and two-body densities in order to extract the spatial structure of the DNN bound state. We, first, define the one-body densities as

$$\begin{aligned} \rho_N(r) &= \langle \Psi | \sum_{i=1,2} \delta^3(|\mathbf{r}_i - \mathbf{R}_G| - r) | \Psi \rangle, \\ \rho_D(r) &= \langle \Psi | \delta^3(|\mathbf{r}_D - \mathbf{R}_G| - r) | \Psi \rangle, \\ \rho_T(r) &= \rho_N(r) + \rho_D(r), \end{aligned}$$

where \mathbf{R}_G is the center-of-mass coordinate of the three-body system. The one-body densities represent the probability of finding N , D , or any of them at distance r from the center of mass of the system. We also define the two-body correlation densities as

$$\begin{aligned} \rho_{NN}(x) &= \langle \Psi | \delta^3(|\mathbf{r}_1 - \mathbf{r}_2| - x) | \Psi \rangle, \\ \rho_{DN}(x) &= \langle \Psi | \sum_{i=1,2} \delta^3(|\mathbf{r}_D - \mathbf{r}_i| - x) | \Psi \rangle, \end{aligned}$$

which stand for the probabilities of finding a NN or DN pair at relative distance x . The root-mean-square radius of particle X , $\sqrt{\langle r^2 \rangle_X}$, and relative distance of particles X and Y , R_{XY} , are given as the second moment of the one-body and two-body densities, respectively,

$$\langle r^2 \rangle_X = \int d^3\mathbf{r} r^2 \rho_X(r), \quad R_{XY}^2 = \int d^3\mathbf{x} x^2 \rho_{XY}(x).$$

In this setup, since the imaginary part of the DN potential is not included, the Λ_c^* appears as a stable bound state. Thus, in the variational approach, the DNN three-body bound state can be found in the energy region below the Λ_c^*N threshold $\sqrt{s} \sim 3536$ MeV. If the three-body (quasi-)bound state exists above the Λ_c^*N threshold, the variational calculation will find the Λ_c^*N two-body scattering state as the ground state of the three-body system.

A three-body bound state above the $\pi\Lambda_c N$ threshold $\sqrt{s} \sim 3363$ MeV has a mesonic decay width. The three-body decay width can be estimated by the matrix element of the imaginary part of the DN potential as

$$\Gamma_{\pi Y_c N} = -2\langle\Psi|\text{Im}\hat{V}_{DN}|\Psi\rangle,$$

where $|\Psi\rangle$ is the obtained wave function of the ground state. As seen in Fig. 2, the imaginary part of the DN potential is much smaller than the real part. This may justify the perturbative treatment of the imaginary part, which ignores the dispersive effect on the energy of the DNN system from the imaginary part.

V. RESULTS

A. Quasibound states in the FCA approach

We, first, study the quasibound state found in the FCA calculation. In Figs. 9 and 10 we show the results for $|T|^2$ as functions of the total energy \sqrt{s} assuming the NN system to have reduced size. For both $I_{NN} = 0$, $I_{NN} = 1$ ($J = 1$, $J = 0$), we obtain a neat peak. The resonance energy for $J = 0$ is about 3486 MeV and the width is extremely small. In the case of $J = 1$ we have a smaller binding and the energy is about 3500 MeV, with a width of around 9 MeV. We should note that the binding is similar for both the spin channels. The position of the peak in this approximation is, in a rough estimate, given by the position of the pole of the $\Lambda_c(2595)$. This gives the value of s_1 and, through Eqs. (11) and (12), the value of s .

However, one should note the different strength of $|T|^2$ in these two cases, but a direct comparison cannot be done because the strength of the resonance amplitude at the peak

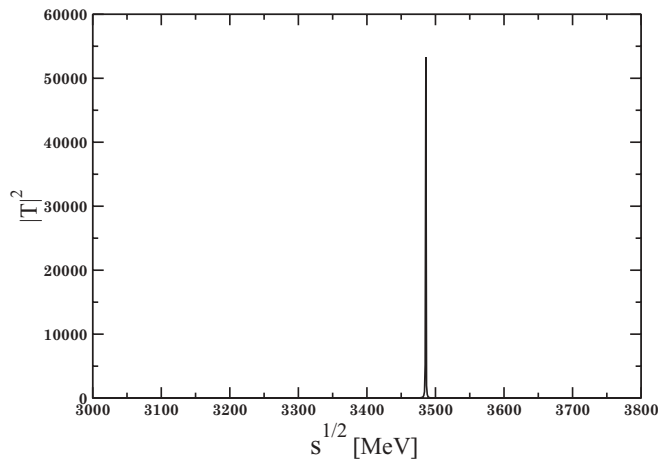


FIG. 9. Modulus-squared of the three-body scattering amplitude for $I = 1/2$ and $J = 0$ with reduced size of the NN radius.

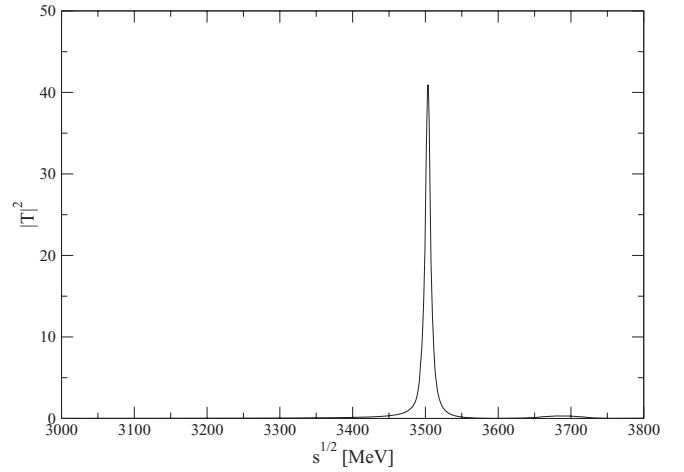


FIG. 10. Modulus-squared of the three-body scattering amplitude for $I = 1/2$ and $J = 1$ with reduced size of the NN radius.

is related to the width, which strongly depends on the spin. A proper comparison is better done after the D absorption is included where the widths are similar.

We next include the $\delta\tilde{g}$ to account for absorption and plot $|T|^2$ for the DNN system in Figs. 11 and 12 for $J = 0$ ($I_{NN} = 1$) and $J = 1$ ($I_{NN} = 0$). The difference of the peak position by the absorption effect is only a few MeV (2–4 MeV) which is certainly within our uncertainties. The novelty, which is welcome, is that $|T|^2$ has become now wider and acquires a width of about 20–25 MeV. We are now in a position to compare the strength of these two amplitudes and we see that, in the case of $J = 0$, the strength of $|T|^2$ at the peak is about a factor 15 larger than that for $J = 1$. This means that the state that we find at $J = 1$ should be more difficult to see, or alternatively we should see the small strength as an indication that this state is more uncertain in our approximation, as should be the smaller shoulder that one can see at higher energies for $J = 1$ in Fig. 12.

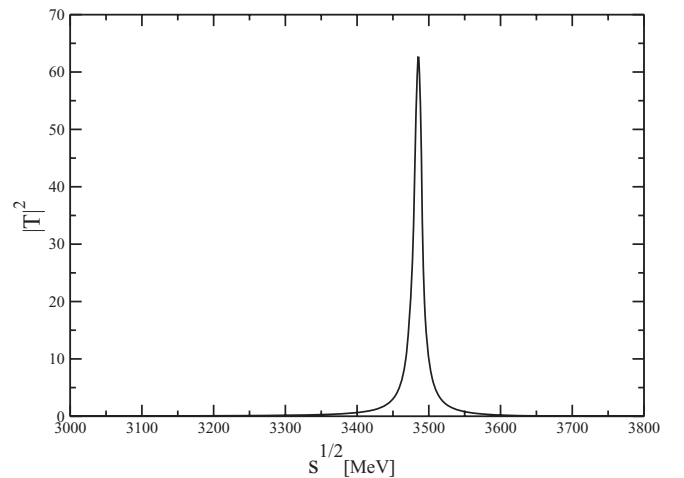


FIG. 11. Modulus-squared of the three-body scattering amplitude for $I = 1/2$ and $J = 0$ (with $\delta\tilde{g}$) with reduced NN radius.

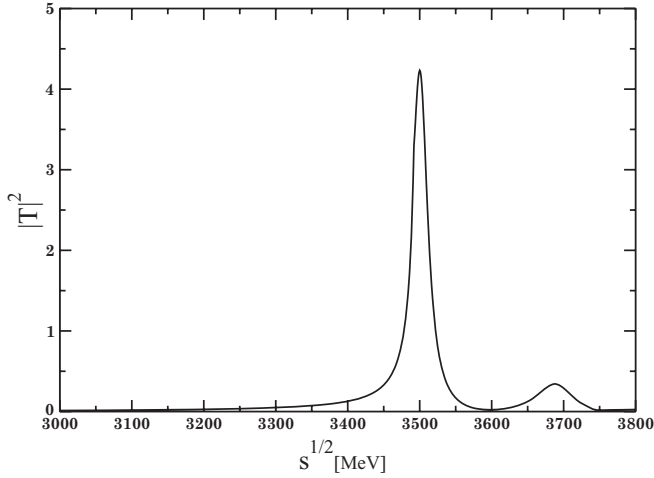


FIG. 12. Modulus-squared of the three-body scattering amplitude for $I = 1/2$ and $J = 1$ (with $\delta\tilde{G}$) with reduced NN radius.

B. Quasibound states in the variational approach

Now we investigate the same system in the variational approach. We, first, adopt the HN1R potential for the nuclear force. As a result of the variational calculation, we have found that the total spin $J = 1$ system ($I_{NN} = 0$) is unbound with respect to the Λ_c^*N threshold. A bound state of the spin $J = 0$ system ($I_{NN} = 1$) is found at

$$B \sim 225 \text{ MeV},$$

measured from the DNN threshold (~ 3745 MeV). This corresponds to the total energy of the three-body system as

$$M_B \sim 3520 \text{ MeV}.$$

We also examine the Minnesota force and Av18 potential. The results are summarized in Table I, together with the contributions from the individual terms in Eq. (18).

As seen in the Table I, the DNN system in the $J = 0$ channel is bound below the Λ_c^*N threshold ($B \sim 209$ MeV)

TABLE I. Results of the energy compositions in the variational calculation for the ground state of the DNN system with total isospin $I = 1/2$ (range parameter $a_s = 0.4$ fm). Terms *bound* and *unbound* are defined with respect to the Λ_c^*N threshold. All the numbers are given in MeV.

	HN1R $J = 1$	$J = 0$	Minnesota $J = 0$	Av18 $J = 0$
B	Unbound	Bound	Bound	Bound
M_B	208	225	251	209
$\Gamma_{\pi Y_c N}$	—	26	38	22
E_{kin}	338	352	438	335
$V(NN)$	0	-2	19	-5
$V(DN)$	-546	-575	-708	-540
T_{nuc}	113	126	162	117
E_{NN}	113	124	181	113
$P(\text{odd})$	75.0%	14.4%	7.4%	18.9%

for all the NN potentials employed.¹ A large kinetic energy of the deeply bound system is overcome by the strong attraction of the DN potential, while the NN potential adds a small correction. Comparing the results with three different nuclear forces, we find that the binding energy is smaller when the NN potential has a harder repulsive core (see Appendix A).

In the $J = 1$ channel, the ground-state energy is obtained slightly above the Λ_c^*N threshold. The fact that the $J = 1$ channel is unbound is confirmed by changing the parameter μ in the trial wave function, which controls the size of the total system [30]. By increasing the system size, the total energy gradually approaches the Λ_c^*N threshold. This indicates that the lowest-energy state is indeed a two-body scattering state of the Λ_c^*N channel. A large fraction of the odd component in this channel ($\sim 75\%$) is realized to enhance the $I_{NN} = 1$ component which has larger fraction of the $I_{DN} = 0$ than the $I_{NN} = 0$ component. In fact, pure $(DN)_{I=0}N$ state can be decomposed into $I_{NN} = 0$ and $I_{NN} = 1$ components with the ratio 1:3. Since the $I_{NN} = 1$ state is the odd state in $J = 1$ ($S_{NN} = 1$) channel, the 75% fraction of the odd component indicates that the DN pair forms the Λ_c^* . We also examine the $J = 1$ channel with the Minnesota force. Although the repulsive core is soft in this case, no bound Λ_c^*N is found.

Using the imaginary part of the DN potential, we evaluate the mesonic decay width of the quasibound state in the $J = 0$ channel, $\Gamma_{\pi Y_c N}$. The results are 20–40 MeV as shown in Table I. This corresponds to the result of FCA without the D absorption, where the width is less than 10 MeV. Note, however, that, in the variational approach, we have evaluated the width perturbatively, while in the FCA the evaluation is done nonperturbatively. In this sense, $\Gamma_{\pi Y_c N}$ obtained in the variational approach can only be regarded as an estimation of the mesonic decay width.

C. Structure of the DNN quasibound state

To further investigate the structure of the DNN systems, we calculate the expectation values of various distances of the obtained wave function. The results of the root-mean-square radii and the relative distances are shown in Table II. Except for the Av18 case where the wave function spreads due to the weaker binding, the size of the DNN bound state in the $J = 0$ channel is smaller than the $\bar{K}NN$ system, in which the NN and $\bar{K}N$ distances are $R_{NN} \sim 2.2$ fm and $R_{\bar{K}N} \sim 1.9$ fm. It is, on the other hand, acceptable to use the reduced size of Eq. (10) for the NN distribution in the FCA calculation, given the uncertainty that arises from the choice of the NN interaction. The large relative distances in the $J = 1$ channel also reflect the nature of the scattering state in this channel.

In view of the different values of R_{NN} obtained from the use of different NN potentials (see Table II) and the different binding obtained in each case (see Table I), we redo the calculations in the FCA changing the NN form factor of Eq. (10). We find a change in the binding from $R_{NN} = 2.62$ fm to 1.55 fm of 10 MeV (more bound) versus 16 MeV in

¹Av18 case is almost at the Λ_c^*N threshold, but we confirm that the wave function is localized as we will see in Sec. VC.

TABLE II. Structure of the DNN ground state (range parameter $a_s = 0.4$ fm). $\sqrt{\langle r^2 \rangle_T}$, $\sqrt{\langle r^2 \rangle_D}$, and $\sqrt{\langle r^2 \rangle_N}$ mean the root-mean-square radius of the distribution of total system, nucleons, and D meson, respectively. R_{NN} (R_{DN}) is the mean distance between two nucleons (D meson and a nucleon) in the DNN . $R_{DN}(I)$ is the mean distance of a DN component with isospin I . All numbers are given in fm.

	HN1R $J = 1$	$J = 0$	Minnesota $J = 0$	Av18 $J = 0$
$\sqrt{\langle r^2 \rangle_T}$	4.81	0.75	0.50	1.26
$\sqrt{\langle r^2 \rangle_N}$	5.61	0.88	0.59	1.47
$\sqrt{\langle r^2 \rangle_D}$	2.52	0.41	0.28	0.67
R_{NN}	10.04	1.55	1.03	2.62
R_{DN}	7.11	1.12	0.76	1.87
$R_{DN}(I = 0)$	4.52	0.83	0.62	1.28
$R_{DN}(I = 1)$	10.03	1.57	1.03	2.65

Table I. In the case of R_{NN} , from $R_{NN} = 2.62$ fm to 1.03 fm the change is 28 MeV (more bound) versus 42 MeV in Table I. The effects of the binding go in the same direction in both cases and they also agree in absolute value at the qualitative level.

In Fig. 13, we show the one-body densities of the nucleon and D meson of the quasibound state with the HN1R potential. It is clear that the D meson distributes more compactly than the nucleons. This result indicates a schematic picture where the D meson sits at the center and nucleons circulate around it.

It is instructive to look at the DN correlation in more detail. In Fig. 14, we show the DN two-body correlation

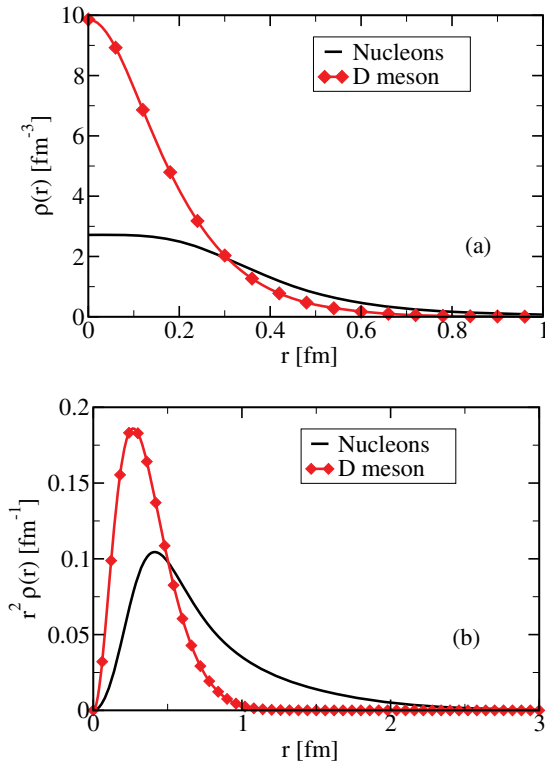


FIG. 13. (Color online) (a) One-body densities $\rho_N(r)$ and $\rho_D(r)$ in the $J = 0$ channel with HN1R potential. (b) The same plot of the densities multiplied by r^2 .

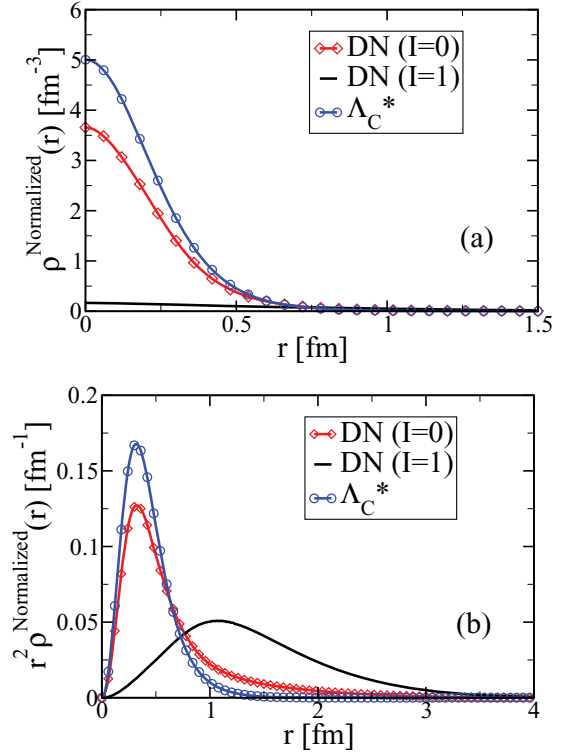


FIG. 14. (Color online) (a) Normalized DN two-body correlation density $\rho_{DN}(r)$ with isospin decomposition. The $I = 0$ DN bound state (Λ_c^*) correlation density is also shown for comparison. (b) The same plot of the densities multiplied by r^2 .

density as well as its isospin decomposition. It is seen that the $I = 0$ component distributes more compactly than the $I = 1$ component, which reflects the strength of the attraction in each channel [see Eq. (19)]. Moreover, the $I = 0$ component is similar to the distribution of the relative distance of the DN two-body bound state $\rho_{\Lambda_c^*}(r)$. This indicates that the structure of the Λ_c^* is maintained even in the three-body system. This feature has also been found in the $\bar{K}NN$ system [30,67].

As in the case of the $\bar{K}NN$ system, the survival of the Λ_c^* in the three-body system opens the possibility of the “ Λ_c^* -hypernuclei,” in which the Λ_c^* is treated as an effective degree of freedom [68,69]. In fact, this picture is more suitable in the charm sector, since the width of the Λ_c^* is smaller than that of the Λ^* , so the effect of the imaginary part in the calculation should be smaller. Note also that the binding of the DN system is as large as 200 MeV, while the binding of the Λ_c^*N is much smaller, especially for the case of the realistic Av18 potential.

We have examined theoretical uncertainties in the construction of the potential. The range parameter of the DN potential a_s is introduced in Eq. (5) and chosen to be 0.4 fm. When we adopt $a_s = 0.35$ fm, the binding energy changes by a few MeV, and the size changes less than 0.1 fm. The Minnesota potential has a parameter u which controls the strength of the NN odd force [65]. The effect of the slight inclusion of the odd force ($u = 0.95$) turns out to be very small, less than 1 MeV. We thus conclude that these uncertainties are much smaller than the dependence on the choice of the NN potential. The

variation of the values in Tables I and II can be regarded as the theoretical uncertainties in the present calculation.

VI. DISCUSSION

A. Comparison of two approaches

We have presented the results of two approaches, the Faddeev FCA calculation and the variational calculation. In the total spin $J = 0$ channel, both approaches find a quasibound state around 3500 MeV, which is below the Λ_c^*N threshold. The assumed NN distribution in the FCA turns out to be similar with that found in the variational calculation by minimizing the total energy. It is, therefore, reasonable to conclude that these approaches find the same quasibound state.

The spin $J = 1$ channel, on the other hand, has differences in the two approaches. The lowest-energy state obtained in the variational calculation is a Λ_c^*N scattering state, while a narrow peak is found in the FCA amplitude below the Λ_c^*N threshold, although the signal strength is not so significant as in the $J = 0$ case. A major reason of this discrepancy may be traced back to the DN interaction in the isospin $I = 1$ channel. In the original coupled-channels amplitude, there is an $I = 1$ quasibound state, which induces the bound state in the FCA. As discussed in Sec. II B, however, the energy dependence of the DN potential in the variational approach is fixed at the energy of the Λ_c^* in the $I = 0$ channel. This reduces the strength of the $I = 1$ amplitude, and the two-body quasibound state is not generated in the effective potential. Since the total spin $J = 1$ channel has larger fraction of the $I = 1$ DN amplitude, this difference is enhanced and results in different three-body results.

In fact, we may artificially adjust the condition Eq. (19) to generate a quasibound state in the $I = 1$ channel in the variational approach. By setting the strength of the DN interaction at $W \sim 2766$ MeV in the $I = 1$ channel, a quasibound state is generated in the $I = 1$ DN channel. In this case, the energy dependence of the DN interaction is fixed at each isospin channel, and the strength of the DN attraction is increased in the $I = 1$ channel. By performing the three-body calculation, we find that the binding energy in the $J = 0$ quasibound state are increased by 10–50 MeV, depending on the NN interaction employed. This is because of the increase of the attraction, and the binding energy appears to be closer to the FCA result. In the $J = 1$ sector, only the Minnesota potential supports a bound state with $B = 214$ MeV, while no state is found below the Λ_c^*N threshold with the other two NN interactions. Given the uncertainty in the choice of the NN interaction, the present result does not strongly support the existence of the quasibound state in the $J = 1$ sector. In order to pin down the $J = 1$ quasibound state, it is necessary to accumulate the experimental information of the DN $I = 1$ scattering amplitude or the information on the negative parity Σ_c^* resonance.

The difference of the results in two approaches also stems from the odd component of the NN state, which is included only in the variational calculation. For a bound state, the inclusion of additional components in the wave function generally increases the binding energy. In fact, when the odd component is switched off, we obtain $B \sim 211$ MeV for the $J = 0$ case with the Minnesota potential. Thus, for the

TABLE III. Binding energies of the three-body bound state in $J = 0$ channel measured from the three-body threshold with different meson mass and different meson-nucleon potential.

	$m = m_{\bar{K}}$	$m = m_D$
$V = V_{\bar{K}}$	~ 30 MeV	~ 190 MeV
$V = V_D$	~ 40 MeV	~ 230 MeV

$J = 0$ quasibound state, we consider that the effect of the odd component is comparable with the uncertainty from the NN force. For the $J = 1$ case, the odd component may be more important, because we need 3/4 fraction of the odd component to obtain a pure Λ_c^*N scattering state. This may be related with the discrepancy of the results in the $J = 1$ channel.

In addition, we should also remember that the two approaches employ different approximations. In the FCA, the dynamics of the nucleons is not solved explicitly, while the imaginary part of the DN potential is not taken into account in the variational approach. In both cases, the explicit $\pi Y_c N$ dynamics is approximated at different levels (see the discussion in Ref. [36]), whereas its importance has been pointed out in the strangeness sector [31]. These effects can also be responsible for the difference of the results in the two approaches.

B. Comparison with $\bar{K}NN$ results

It is instructive to compare the DNN quasibound state with the corresponding $\bar{K}NN$ state in Ref. [30]. In both cases, we obtain a quasibound state, but the DNN system has a larger binding energy and a narrower width. This is in parallel with the properties of the DN and $\bar{K}N$ two-body quasibound states, and they are closely related through the DN and $\bar{K}N$ interactions.

As discussed in Sec. II A, the D meson can be more strongly bound in a nucleus than \bar{K} meson by two reasons. On the one hand, the coupling itself is stronger, and, on the other hand, the heavier mass of the D meson is advantageous to increase the binding. So, we can consider two hypothetical variants between the DNN system ($B \sim 230$ MeV) and $\bar{K}NN$ system ($B \sim 30$ MeV)²: case I, with kinematics of the DNN system with the $\bar{K}N$ potential ($m = m_D$, $V = V_{\bar{K}}$), and case II, with kinematics of the $\bar{K}NN$ system with the DN potential ($m = m_{\bar{K}}$, $V = V_D$). The result of the variational calculation shows that $B \sim 40$ MeV for case I and $B \sim 190$ MeV for case II. As summarized in Table III, the suppression of the kinetic energy by the heavy D mass is more important for the strong binding of the DNN system. One should note that, in the present case, the strength of the two-body interaction is fixed at the energy of the two-body quasibound state. Since the DN two-body bound state locates 200 MeV below the DN threshold, the strength of the potential is reduced, as seen in Fig. 1. Thus, in the present prescription, the attractive strength of the DN potential does not differ much from the $\bar{K}N$ one, and the result of case I does not very much deviate from the $\bar{K}NN$ quasibound state.

²Here we also set the strength of the $\bar{K}N$ potential at the energy of the Λ_c^* for comparison with the DNN calculation.

The narrow width of the DNN system is a consequence of the narrow width of the $\Lambda_c^*(2595)$. This is partly because of the small transition coupling which is suppressed by the exchange of the heavy flavor, but the main reason is the suppression of the phase space due to the large binding energy. In this sense, the heaviness of the D meson is essential to realize the deep and narrow DNN quasibound state.

C. Possible experiments to produce the DNN state

The very narrow width of the DNN system differs qualitatively from the $\bar{K}NN$ one, where the width was so large as to make its experimental observation unfeasible. In the present case, there is a clear situation and there are no problems, in principle, for the observation of the state. In the FCA calculation, we observe that the two-nucleon absorption width is larger than the three-body decay width. This indicates that the DNN quasibound state can be more easily seen in the two-baryon final states such as $\Lambda_c N$. The findings of the present work should stimulate efforts to find suitable reactions where this state could be found.

As a suggestion in this direction we can think of the $\bar{p}^3\text{He} \rightarrow \bar{D}^0 D^0 pn \rightarrow \bar{D}^0[DNN]$ reaction, which could be done by the GSI Facility for Antiproton and Ion Research (FAIR). With a \bar{p} beam of 15 GeV/c, there is plenty of energy available for this reaction and the momentum mismatch of the D^0 with the spectator nucleons of the ^3He can be of the order of 550 MeV/c, equivalent to an energy of 80 MeV for the D , small compared with the scale of the binding ($\gtrsim 200$ MeV). With an estimate of $\sigma \simeq 10\text{--}20$ nb for $\bar{p}p \rightarrow \bar{D}^0 D^0$ production [70,71], one would expect several thousand events per day for the background of the proposed reaction [72]. A narrow peak could be visible on top of this background corresponding to the DNN bound-state formation.

Another possibility is the high-energy π -induced reaction. An analogous reaction is $\pi^- d \rightarrow D^- D^+ np \rightarrow D^- [DNN]$, where the relevant elementary process is $\pi^- N \rightarrow D^+ D^- N$. Since the DN pair in the DNN system is strongly clustering as the Λ_c^* , the reaction $\pi^- d \rightarrow D^- \Lambda_c^* n \rightarrow D^- [DNN]$ is also another candidate. The elementary reaction $\pi^- p \rightarrow D^- \Lambda_c^*$ is relevant in this case. Such reactions may be realized in the high-momentum beamline project at Japan Proton Accelerator Research Complex (J-PARC).

A different strategy is to look for the formation of the quasibound state in heavy-ion collisions. It has been shown that the hadronic molecular states with charm quark are abundantly produced at Relativistic Heavy Ion Collider (RHIC) and Large Hadron Collider (LHC) [73,74]. Although a deeply bound DNN state has a smaller production yield, it can also be produced *via* coalescence of the $\Lambda_c^* N$ with much smaller binding. A peak structure of the DNN state may be seen, for instance, in the invariant mass spectrum of the $\Lambda_c \pi^- p$ or $\Lambda_c p$ final state.

VII. CONCLUSIONS

We have studied the DNN system with $I = 1/2$ and have found that the system is bound and rather stable, with a width of about 20–40 MeV. We obtained a clear signal of the quasibound state for the total spin $J = 0$ channel around 3500 MeV.

We have used two methods for the evaluation of the quasibound state. The first one used the fixed center approximation for the Faddeev equations and the second one employs the variational approach with hadronic potentials in coordinate space. The DN interaction was constructed in the field theoretical method with channel couplings, and a unitary approach dynamically generates the $\Lambda_c^*(2595)$ resonance as a DN quasibound state.

In both cases, we have found a bound state with an energy around 3500 MeV in the $J = 0$ channel. This corresponds to 250 MeV binding from the DNN threshold. The $J = 1$ channel is more subtle, and the precise DN amplitude in the $I = 1$ channel is important for a robust prediction in this channel. The mesonic decay width of the quasibound state turned out to be less than 40 MeV. In addition, the D absorption on two nucleons was evaluated in the FCA formalism. Although the absorption process adds several tens of MeV to the width, the total width is still much smaller than the binding energy. It is found that the DN pair in the $I = 0$ channel in the DNN system resembles the wave function of the $\Lambda_c(2595)$ state in vacuum. Thus, the DNN state found here can be interpreted as a quasibound state of $\Lambda_c(2595)$ and a nucleon.

The small width of the DNN quasibound state is advantageous for the experimental identification. The search for the DNN quasibound state can be done by a \bar{p} -induced reaction at FAIR, a π^- -induced reaction at J-PARC, and relativistic heavy-ion collisions at RHIC and LHC.

ACKNOWLEDGMENTS

This work is partly supported by projects FIS2011-28853-C02-01 from the Ministerio de Ciencia e Innovación (Spain), FEDER funds, and by the Generalitat Valenciana in the program Prometeo/2009/090. This research is part of the European Community-Research Infrastructure Integrating Activity “Study of Strongly Interacting Matter” (acronym Hadron-Physics3, Grant No. 283286) under the Seventh Framework Programme of EU. T.H. thanks the support from the Global Center of Excellence Program by MEXT, Japan, through the Nanoscience and Quantum Physics Project of the Tokyo Institute of Technology. This work is partly supported by the Grant-in-Aid for Scientific Research from MEXT and JSPS (No. 24105702 and No. 24740152). M. Bayar acknowledges support through the Scientific and Technical Research Council (TUBITAK) BIDEP-2219.

APPENDIX A: NN INTERACTIONS

Here we summarize the properties of the NN potentials used in this study with a variational calculation. We have examined three kinds of NN interactions. Because we work in the isospin symmetric limit, the Coulomb interaction is not included in all cases.

The Hasegawa-Nagata No. 1 potential [64] has a three-range Gaussian form with no odd force. The repulsive core is as high as 1 GeV. Because the potential was originally introduced for the resonating-group-method study, when applied to the two-nucleon systems, the attraction is too strong to generate a bound state in the 1S_0 channel and to overestimate the deuteron

binding energy. In this study, we have reduced the strength of the long-range term (middle-range term) by factor 0.25 (0.95) and call it the HN1R potential. The HN1R potential has no bound state in the 1S_0 channel and reproduces the NN phase-shift data, as shown below.

Minnesota force [65] is expressed by the sum of two Gaussians, with a relatively soft repulsive core. The parameters were chosen so as to reproduce the scattering lengths and the effective ranges of the NN scattering. As a consequence, the deuteron is bound only with the s -wave component, so the tensor force is considered to be renormalized in the central part. We set the parameter $u = 1$ so there is no odd force, unless otherwise stated.

The Argonne v18 potential [66] is one of the realistic nuclear forces with a strong repulsive core. As in Ref. [30], we used the Gaussian-fitted version of the potential with central, spin-spin, and L^2 terms. Since the description of the deuteron requires d -wave mixing, which is beyond the present model wave function, we only consider the $S = 0$ channel with the Av18 potential.

In Fig. 15, we show the spatial form of the potentials in the 1S_0 channel. The phase shifts of the NN scattering in the 1S_0 channel are shown in Fig. 16 in comparison with experimental data.

APPENDIX B: DERIVATION OF THE THREE-BODY AMPLITUDE IN THE CHARGE BASIS

In this Appendix, we derive Eqs. (8) and (9) in the Approach of Ref. [36] by applying the following strategy.

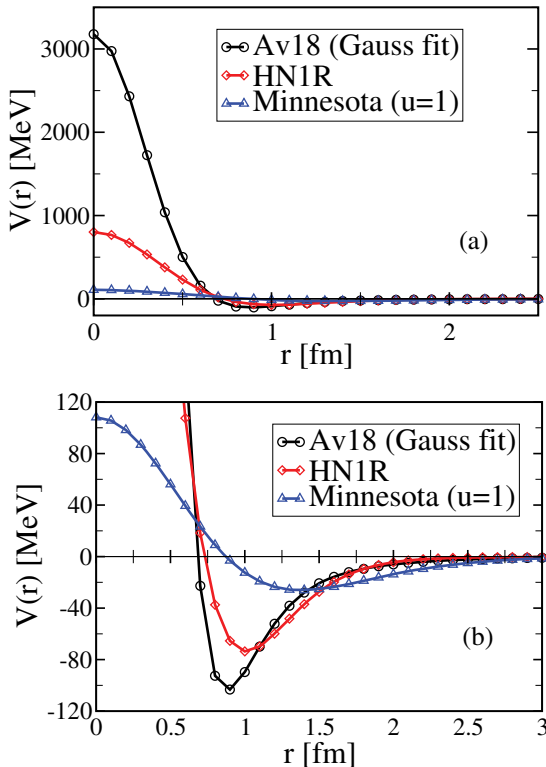


FIG. 15. (Color online) (a) Coordinate space NN potentials in the 1S_0 channel. (b) Detail of the lower part of (a).

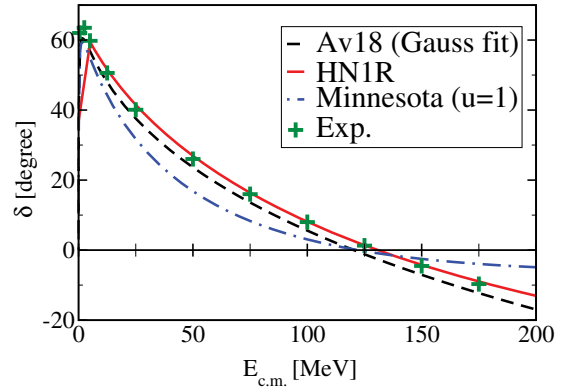


FIG. 16. (Color online) NN phase shifts in the 1S_0 channel calculated by the NN potentials.

We evaluate, first, the $D^0 pp \rightarrow D^0 pp$ amplitude considering charge exchange processes in the rescattering of the D meson. The amplitude will contain total isospin $I_{\text{tot}} = 1/2$ and $I_{\text{tot}} = 3/2$. Since we only want the $I_{\text{tot}} = 1/2$, we evaluate the scattering amplitude for $I_{\text{tot}} = 3/2$ in addition, taking the $D^+ pp \rightarrow D^+ pp$ amplitude, and from a linear combination of the two we obtain the $I_{\text{tot}} = 1/2$ amplitude. This strategy was found most practical in Ref. [36].

For the $D^0 pp \rightarrow D^0 pp$ we define three components of the three-body scattering amplitude as follows:

- (i) T_p , which are called partition functions, which contains all diagrams that begin with a D^0 collision with the first proton of the pp system and finish with $D^0 pp$,
- (ii) $T_{\text{ex}}^{(p)}$, which contains all the diagrams that begin with a $D^+ p$ collision on a np system and finish with $D^0 pp$, and
- (iii) $T_{\text{ex}}^{(n)}$, which contains all the diagrams that begin with a $D^+ n$ collision on a np system and finish with $D^0 pp$.

These amplitudes fulfill a set of coupled equations,

$$\begin{aligned} T_p &= t_p + t_p G_0 T_p + t_{\text{ex}} G_0 T_{\text{ex}}^{(p)} \\ T_{\text{ex}}^{(p)} &= t_0^{(p)} G_0 T_{\text{ex}}^{(n)} \\ T_{\text{ex}}^{(n)} &= t_{\text{ex}} + t_{\text{ex}} G_0 T_p + t_0^{(n)} G_0 T_{\text{ex}}^{(p)}, \end{aligned} \quad (\text{B1})$$

where the two-body amplitudes are given as $t_p = t_{D^0 p, D^0 p}$, $t_{\text{ex}} = t_{D^0 p, D^+ n}$, $t_0^{(p)} = t_{D^+ p, D^+ p}$, and $t_0^{(n)} = t_{D^+ n, D^+ n}$. The set of equations (B1) are diagrammatically represented in Fig. 17.

By taking into account the phase convention $|D^0\rangle = -|1/2, -1/2\rangle$ in the isospin basis, we can write all the former elementary amplitudes in terms of $I = 0, 1$ [$t^{(0)}, t^{(1)}$] for the DN system, and we find

$$\begin{aligned} t_p &= \frac{1}{2}[t^{(0)} + t^{(1)}] & t_{\text{ex}} &= \frac{1}{2}[t^{(0)} - t^{(1)}] \\ t_0^{(p)} &= t^{(1)} & t_0^{(n)} &= \frac{1}{2}[t^{(0)} + t^{(1)}]. \end{aligned} \quad (\text{B2})$$

Eliminating $T_{\text{ex}}^{(p)}$ and $T_{\text{ex}}^{(n)}$ in Eq. (B1) we obtain

$$T_p = \frac{t_p(1 - t_0^{(n)} G_0 t_0^{(p)} G_0) + t_{\text{ex}}^2 G_0 t_0^{(p)} G_0}{(1 - t_p G_0)[1 - t_0^{(n)} G_0 t_0^{(p)} G_0] - t_{\text{ex}}^2 t_0^{(p)} G_0^3}, \quad (\text{B3})$$

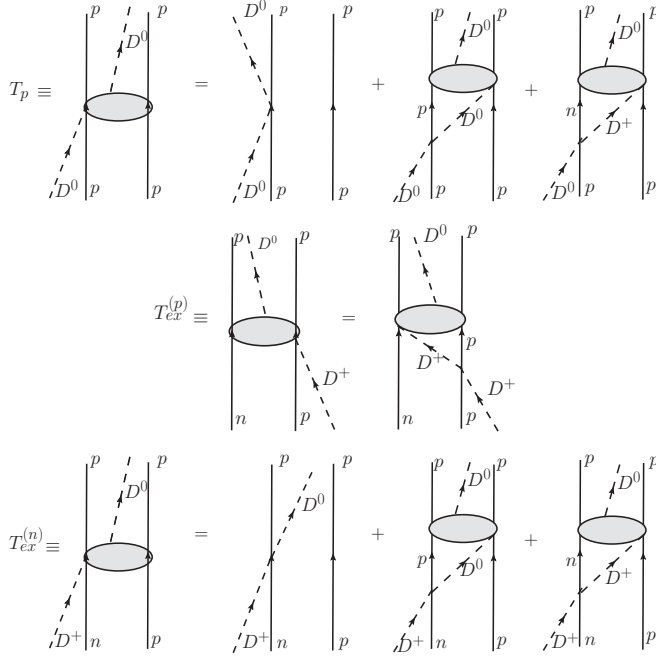


FIG. 17. Diagrammatic representations of the partition functions for the $D^0 pp \rightarrow D^0 pp$.

which, in the isospin basis, can be simplified to

$$T_p = \frac{\frac{1}{2}[t^{(0)} + t^{(1)}] - t^{(0)}t^{(1)^2}G_0^2}{[1 - G_0t^{(1)}]\{1 + \frac{1}{2}[t^{(1)} - t^{(0)}]G_0 - G_0^2t^{(0)}t^{(1)}\}}.$$

The total $D^0 pp \rightarrow D^0 pp$ amplitude would be $2T_p$, accounting for the first interaction of the D^0 with either of the protons.

We now take into account that, in the basis of $|I_{\text{tot}}, I_{3,\text{tot}}\rangle$,

$$|D^0 pp\rangle = -\left(\frac{1}{\sqrt{3}}|3/2, 1/2\rangle + \sqrt{\frac{2}{3}}|1/2, 1/2\rangle\right) \quad (\text{B4})$$

and, thus,

$$\langle 1/2|T|1/2\rangle = \frac{3}{2}(\langle D^0 pp|T|D^0 pp\rangle - \frac{1}{3}\langle 3/2|T|3/2\rangle). \quad (\text{B5})$$

The $\langle 3/2|T|3/2\rangle$ amplitude is particularly easy to obtain. In this case, we take the $D^+ pp \rightarrow D^+ pp$ transition and, diagrammatically, we have the mechanism of Fig. 18 for the only partition function $T_p^{(3/2)}$.

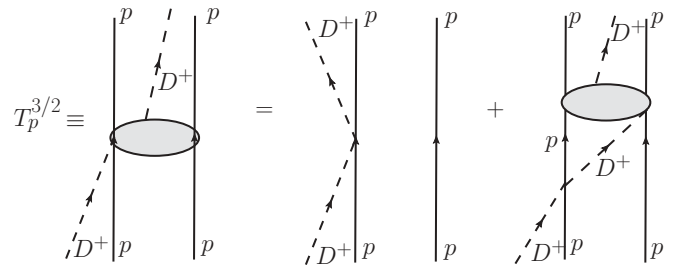


FIG. 18. Diagrammatic representation of the partition function for $I = 3/2$.

Hence,

$$T_p^{(3/2)} = t_0^{(p)} + t_0^{(p)}G_0T_p^{(3/2)} \quad (\text{B6})$$

and the total $T^{(3/2)}$ amplitude will be $2T_p^{(3/2)}$, accounting for the D^+ interacting first also with the second nucleon. We have

$$T_p^{(3/2)} = \frac{t_0^{(p)}}{1 - G_0t_0^{(p)}} = \frac{t^{(1)}}{1 - G_0t^{(1)}}. \quad (\text{B7})$$

We can now use Eq. (B5) and find for the total amplitude (including the factor 2 for the first interaction with either proton)

$$\begin{aligned} T^{(1/2)} &= 3T_p - \frac{t^{(1)}}{1 - G_0t^{(1)}} \\ &= \frac{\frac{3}{2}t^{(0)} + \frac{1}{2}t^{(1)} - \frac{1}{2}t^{(1)}(t^{(1)} - t^{(0)})G_0 - 2t^{(0)}t^{(1)^2}G_0^2}{[1 - G_0t^{(1)}]\{1 + \frac{1}{2}[t^{(1)} - t^{(0)}]G_0 - G_0^2t^{(0)}t^{(1)}\}}, \end{aligned}$$

which can be simplified by dividing the numerator by $[1 - G_0t^{(1)}]$ with the final result,

$$T^{(1/2)} = \frac{\frac{3}{2}t^{(0)} + \frac{1}{2}t^{(1)} + 2G_0t^{(0)}t^{(1)}}{1 + \frac{1}{2}[t^{(1)} - t^{(0)}]G_0 - G_0^2t^{(0)}t^{(1)}}.$$

This corresponds to Eq. (8).

The case of $S_{NN} = 1$ ($I_{NN} = 0$), that we also study here, can be done in a similar way, but this was done in Ref. [48] for K^-d at rest and in Ref. [35] for the K^-d interaction below threshold. We quote here the formula that was obtained in Ref. [35] which we use here, too,

$$T_{D^0d} = \frac{\frac{1}{2}t^{(0)} + \frac{3}{2}t^{(1)} + 2G_0t^{(0)}t^{(1)}}{1 - \frac{1}{2}[t^{(1)} - t^{(0)}]G_0 - G_0^2t^{(0)}t^{(1)}}.$$

This corresponds to Eq. (9).

- [1] M. Krell and T. E. O. Ericson, *Nucl. Phys. B* **11**, 521 (1969).
 [2] H. Toki, S. Hirenzaki, T. Yamazaki, and R. S. Hayano, *Nucl. Phys. A* **501**, 653 (1989).
 [3] J. Nieves, E. Oset, and C. Garcia-Recio, *Nucl. Phys. A* **554**, 509 (1993).
 [4] C. J. Batty, E. Friedman, and A. Gal, *Phys. Rep.* **287**, 385 (1997).
 [5] S. Hirenzaki, Y. Okumura, H. Toki, E. Oset, and A. Ramos, *Phys. Rev. C* **61**, 055205 (2000).

- [6] R. S. Hayano and T. Hatsuda, *Rev. Mod. Phys.* **82**, 2949 (2010).
 [7] S. Hirenzaki, H. Toki, and T. Yamazaki, *Phys. Rev. C* **44**, 2472 (1991).
 [8] J. Nieves and E. Oset, *Phys. Lett. B* **282**, 24 (1992).
 [9] K. J. Raywood, J. B. Lange, G. Jones, M. Pavan, M. E. Sevior, D. A. Hutcheon, A. Olin, D. Ottewell *et al.*, *Phys. Rev. C* **55**, 2492 (1997).
 [10] M. Lutz, *Phys. Lett. B* **426**, 12 (1998).

- [11] A. Ramos and E. Oset, *Nucl. Phys. A* **671**, 481 (2000).
- [12] J. Schaffner-Bielich, V. Koch, and M. Effenberger, *Nucl. Phys. A* **669**, 153 (2000).
- [13] A. Cieply, E. Friedman, A. Gal, and J. Mares, *Nucl. Phys. A* **696**, 173 (2001).
- [14] E. Friedman, A. Gal, and C. J. Batty, *Nucl. Phys. A* **579**, 518 (1994).
- [15] A. Baca, C. Garcia-Recio, and J. Nieves, *Nucl. Phys. A* **673**, 335 (2000).
- [16] V. K. Magas, E. Oset, A. Ramos, and H. Toki, *Phys. Rev. C* **74**, 025206 (2006).
- [17] E. Oset, V. K. Magas, A. Ramos, and H. Toki, *The 9th International Conference on Hypernuclear and Strange Particle Physics, 10–14 Oct 2006, Mainz, Germany*, edited by T. Walcher (Springer, Berlin, HYP 2006).
- [18] R. H. Dalitz and S. F. Tuan, *Phys. Rev. Lett.* **2**, 425 (1959); *Ann. Phys.* **10**, 307 (1960).
- [19] N. Kaiser, P. B. Siegel, and W. Weise, *Nucl. Phys. A* **594**, 325 (1995).
- [20] E. Oset and A. Ramos, *Nucl. Phys. A* **635**, 99 (1998).
- [21] J. A. Oller and U. G. Meissner, *Phys. Lett. B* **500**, 263 (2001).
- [22] M. F. M. Lutz and E. E. Kolomeitsev, *Nucl. Phys. A* **700**, 193 (2002).
- [23] D. Jido, J. A. Oller, E. Oset, A. Ramos, and U. G. Meissner, *Nucl. Phys. A* **725**, 181 (2003).
- [24] T. Hyodo and D. Jido, *Prog. Part. Nucl. Phys.* **67**, 55 (2012).
- [25] Y. Ikeda, T. Hyodo, and W. Weise, *Phys. Lett. B* **706**, 63 (2011); *Nucl. Phys. A* **881**, 98 (2012).
- [26] Y. Ikeda and T. Sato, *Phys. Rev. C* **76**, 035203 (2007).
- [27] N. V. Shevchenko, A. Gal, and J. Mares, *Phys. Rev. Lett.* **98**, 082301 (2007).
- [28] N. V. Shevchenko, A. Gal, J. Mares, and J. Revai, *Phys. Rev. C* **76**, 044004 (2007).
- [29] A. Dote, T. Hyodo, and W. Weise, *Nucl. Phys. A* **804**, 197 (2008).
- [30] A. Dote, T. Hyodo, and W. Weise, *Phys. Rev. C* **79**, 014003 (2009).
- [31] Y. Ikeda and T. Sato, *Phys. Rev. C* **79**, 035201 (2009).
- [32] T. Yamazaki and Y. Akaishi, *Phys. Lett. B* **535**, 70 (2002).
- [33] Y. Ikeda, H. Kamano, and T. Sato, *Prog. Theor. Phys.* **124**, 533 (2010).
- [34] M. Bayar, J. Yamagata-Sekihara, and E. Oset, *Phys. Rev. C* **84**, 015209 (2011).
- [35] E. Oset, D. Jido, T. Sekihara, A. M. Torres, K. P. Khemchandani, M. Bayar, and J. Yamagata-Sekihara, *Nucl. Phys. A* **881**, 127 (2012).
- [36] M. Bayar and E. Oset, *Nucl. Phys. A* **883**, 57 (2012).
- [37] N. Barnea, A. Gal, and E. Z. Liverts, *Phys. Lett. B* **712**, 132 (2012).
- [38] J. Hofmann and M. F. M. Lutz, *Nucl. Phys. A* **763**, 90 (2005).
- [39] T. Mizutani and A. Ramos, *Phys. Rev. C* **74**, 065201 (2006).
- [40] L. Tolos, A. Ramos, and T. Mizutani, *Phys. Rev. C* **77**, 015207 (2008).
- [41] C. Garcia-Recio, V. K. Magas, T. Mizutani, J. Nieves, A. Ramos, L. L. Salcedo, and L. Tolos, *Phys. Rev. D* **79**, 054004 (2009).
- [42] L. Tolos, C. Garcia-Recio, and J. Nieves, *Phys. Rev. C* **80**, 065202 (2009).
- [43] C. Garcia-Recio, J. Nieves, and L. Tolos, *Phys. Lett. B* **690**, 369 (2010).
- [44] T. Sekihara, D. Jido, and Y. Kanada-En'yo, *Phys. Rev. C* **79**, 062201 (2009).
- [45] T. Hyodo and W. Weise, *Phys. Rev. C* **77**, 035204 (2008).
- [46] R. Chand and R. H. Dalitz, *Ann. Phys.* **20**, 1 (1962).
- [47] G. Toker, A. Gal, and J. M. Eisenberg, *Nucl. Phys. A* **362**, 405 (1981).
- [48] S. S. Kamalov, E. Oset, and A. Ramos, *Nucl. Phys. A* **690**, 494 (2001).
- [49] U.-G. Meissner, U. Raha, and A. Rusetsky, *Eur. Phys. J. C* **47**, 473 (2006).
- [50] A. Gal, *Int. J. Mod. Phys. A* **22**, 226 (2007).
- [51] J.-J. Xie, A. Martinez Torres, and E. Oset, *Phys. Rev. C* **83**, 065207 (2011).
- [52] D. Jido and Y. Kanada-En'yo, *Phys. Rev. C* **78**, 035203 (2008).
- [53] A. Martinez Torres, K. P. Khemchandani, and E. Oset, *Phys. Rev. C* **79**, 065207 (2009).
- [54] A. Martinez Torres, and D. Jido, *Phys. Rev. C* **82**, 038202 (2010).
- [55] J.-J. Xie, A. Martinez Torres, E. Oset, and P. Gonzalez, *Phys. Rev. C* **83**, 055204 (2011).
- [56] C. W. Xiao, M. Bayar, and E. Oset, *Phys. Rev. D* **84**, 034037 (2011).
- [57] A. Martinez Torres, E. J. Garzon, E. Oset, and L. R. Dai, *Phys. Rev. D* **83**, 116002 (2011).
- [58] A. Martinez Torres, K. P. Khemchandani, L. S. Geng, M. Napsuciale, and E. Oset, *Phys. Rev. D* **78**, 074031 (2008).
- [59] L. Roca and E. Oset, *Phys. Rev. D* **82**, 054013 (2010).
- [60] R. Machleidt, *Phys. Rev. C* **63**, 024001 (2001).
- [61] E. Oset and A. Ramos, *Nucl. Phys. A* **679**, 616 (2001).
- [62] B. Borasoy, *Phys. Rev. D* **59**, 054021 (1999).
- [63] A. L. Fetter and J. D. Walecka, *Quantum Theory of Many-Particle Systems* (McGraw-Hill, New York, 1971).
- [64] A. Hasegawa and S. Nagata, *Prog. Theor. Phys.* **45**, 1786 (1971).
- [65] D. R. Thompson, M. Lemere, and Y. C. Tang, *Nucl. Phys. A* **286**, 53 (1977).
- [66] R. B. Wiringa, V. G. J. Stoks, and R. Schiavilla, *Phys. Rev. C* **51**, 38 (1995).
- [67] T. Yamazaki and Y. Akaishi, *Phys. Rev. C* **76**, 045201 (2007).
- [68] A. Arai, M. Oka, and S. Yasui, *Prog. Theor. Phys.* **119**, 103 (2008).
- [69] T. Uchino, T. Hyodo, and M. Oka, *Nucl. Phys. A* **868–869**, 53 (2011).
- [70] A. B. Kaidalov and P. E. Volkovitsky, *Z. Phys. C* **63**, 517 (1994).
- [71] A. Khodjamirian, C. Klein, T. Mannel, and Y.-M. Wang, *Eur. Phys. J. A* **48**, 31 (2012).
- [72] U. Wiedner, *Prog. Part. Nucl. Phys.* **66**, 477 (2011).
- [73] S. Cho *et al.* (ExHIC Collaboration), *Phys. Rev. Lett.* **106**, 212001 (2011).
- [74] S. Cho *et al.* (ExHIC Collaboration), *Phys. Rev. C* **84**, 064910 (2011).